Evidence of Progressive Ground Adjustment and Subsurface Flow Reorganisation around Preston New Road

D. Nye
July 26, v1.1

Summary of Observations and Implications

This report documents a series of surface and near-surface ground responses observed across a low-lying drainage and infrastructure corridor surrounding Preston New Road. The findings are based on a structured, multi-source evidence approach combining repeat ground observations, time-series aerial imagery, and LiDAR elevation differencing. These datasets are used to corroborate one another, allowing surface expressions to be assessed in both spatial and temporal context.

Across eleven locations distributed around the Preston New Road corridor, a recurring pattern of ground behaviour has been identified. Observed surface expressions include localised subsidence*, circular depressions, linear cracking, surface mounding, bank erosion, seepage, sediment staining, and progressive reorganisation of surface discharge points. While individual features vary in form and setting, they recur across a connected drainage and infrastructure landscape and exhibit persistence, spatial coherence, and evolution over time. The recurrence of similar surface expressions across multiple locations, land uses, and observation periods supports interpretation of a system-level response rather than coincidental aggregation of isolated defects.

** The term is used descriptively to denote surface lowering, not mechanism*

Importantly, the observations demonstrate that ground response is not confined to open watercourses or agricultural land. Surface expressions are also documented within roadside embankments, pedestrian verges, landscaped public space, junctions, and channel margins, including locations adjacent to residential properties and transport infrastructure. Several features evolve over periods of weeks to months, in some cases responding to changing hydrological conditions, but persisting beyond individual rainfall events or routine seasonal variability, with discharge points appearing, migrating, intensifying, or closing over time. This behaviour is inconsistent with static, incidental, or purely construction-related surface phenomena.

The report does not seek to attribute causation, assign responsibility, or assert the presence of contamination. Instead, it focuses on detectability, interpretation, and system behaviour. The evidence indicates that subsurface water movement and ground adjustment are active and distributed processes within the study area, capable of producing surface expressions that may fall outside conventional monitoring expectations or regulatory classifications.

The findings raise substantive questions regarding the adequacy of existing monitoring frameworks and oversight practices. In particular, they highlight how low-magnitude but evolving features may remain operationally invisible where monitoring prioritises predefined pathways, static conceptual models, or compliance-based thresholds. Where surface expressions are classified narrowly or dismissed in isolation, early indicators of ground and hydrological sensitivity may be overlooked.

This report therefore concludes that confidence in ground stability and drainage performance within the study area cannot be based solely on the absence of threshold exceedance or acute failure. Instead, it depends on the capacity of monitoring and governance systems to recognise and respond to patterns that develop incrementally across space and time, and across multiple land uses and infrastructure types.

The observations presented here are offered to support informed regulatory consideration. They warrant careful review not because they demonstrate harm, but because they demonstrate uncertainty that is active, observable, and evolving. In this context, ‘subsurface flow reorganisation’ is used descriptively to denote changes in the location, timing, or expression of groundwater emergence inferred from surface observations, without implying a specific depth, pathway, or driving mechanism.”

Table Of Contents

1. Introduction 6
1.1 Purpose of submission 6
1.2 Scope of the report 6
1.3 Explicit exclusions and evidential limits 8
2. Methods and data sources 8
2.1 Overview 8
2.2 Aerial and satellite imagery 9
2.3 LiDAR elevation differencing (2018-2022) 9
2.4 Aerial photography (28/01/2026) 9
2.5 Ground-based photography (2018-2026) 9
2.6 Location structure and presentation 9
2.7 Consistency of Figure Selection and Presentation 10
3. Study area overview 10
3.1 - Geographic and hydrological setting 10
3.2 - Surface water behaviour and bank sensitivity 12
3.3 - Relevance to the locations presented 12
4. Locations Overview of Location Framework and Reference Infrastructure 13
Preston New Road Well Pad 13
Main Drain and Catchment Setting 13
4.1 Location 1 13
4.1.1 - Summary of observations (Location 1) 17
4.2 - Location 2 17
4.2.1 Summary of observations (Location 2) 24
4.3 Location 3 24
4.3.1 Summary of observations (Location 3) 33
4.3.2 Closing Statement – Locations 1–3 (Lower and Mid-Corridor Observations) 33
4.4 Location 4 34
4.4.1 - Summary of observations (Location 4) 43
4.5 - Location 5 43
4.5.1 Summary of observations (Location 5) 48
4.6 - Location 6 49
4.6.1 Summary of observations (Location 6) 51
4.6.2 Section Summary - Locations 4 to 6 52
4.7 Location 7 52
4.7.1 Interim Synthesis and Summary - Locations 1-7 55
4.7.2 - Intervening Field between Locations 6 and 7 56
4.7.3 Summary of observations (Location 7) 60

4.8 Location 8 61
Interpretive note (Location 8) 66
4.8.1 - Summary of observations (Location 8) 66
4.9 Location 9 66
4.9.1 Summary of observations (Location 9) 69
4.10 Location 10 70
4.10.1 - Summary of observations (Location 10) 80
4.10.2 - Summary of Locations 8 - 10: Infrastructure-Adjacent and Channel-Connected Ground Response 81
Location 8 81
Location 9 81
Location 10 81
4.11 Location 11 82
4.11.1 - Summary of observations (Location 11) 87
4.12 Location 12 88
4.12.1 Summary of observations (Location 12) 93
5. Discussion and Implications 94
5.1 Implications for Monitoring Design and Sensitivity 95
5.2 Signal Classification and the Risk of False Negatives 96
5.3 Implications for Site-Level Oversight and Ongoing Stability 96
5.4 Governance, Escalation, and Responsibility 97
6. Conclusions 98
6.1 Implications for Regulatory Consideration 99
Appendix A - Location Index and Spatial Referencing 100
A.1 Purpose and Use of This Appendix 100
A.2 Coordinate Reference and Disclaimer 100
Appendix B - Ground Image Log: Location 10 (Main Drain Bank Face) 102
B.1 Purpose of This Log 102
Appendix C - LiDAR Processing Workflow and Interpretation Controls 103
C.1 Purpose of LiDAR Analysis 103
C.2 Data Sources 103
C.3 Pre-processing and Alignment 103
C.4 Elevation Differencing Method 103
C.5 Contour Generation and Interval Selection 103
C.6 Value Masking and Surface Water Considerations 104
C.7 Visualisation Controls 104
C.8 Limitations 104
C.9 Role Within the Evidence Hierarchy 105

C.10 Summary 105
Appendix D: Image Provenance, File Handling, and RAW/JPEG Use 106
D.1 Purpose of Image Documentation 106
D.2 Image Acquisition 106
D.3 RAW and JPEG Image Formats 106
D.4 Image Processing and Handling 106
D.5 RAW-JPEG Differences and Interpretation 107
D.6 Image Selection and Representativeness 107
D.7 Metadata and Traceability 107
D.8 Limitations 107
D.9 Role Within the Evidence Hierarchy 108
D.10 Summary 108
Appendix E: Terminology and Descriptive Language Controls 108
E.1 Purpose of Terminology Controls 108
E.2 Descriptive Versus Interpretive Language 108
E.3 Use of Key Terms 108
E.4 Avoidance of Diagnostic Terminology 109
E.5 Treatment of Ambiguity 109
E.6 Consistency Across Sections 109
E.7 Relationship to Regulatory Interpretation 110
E.8 Summary 110
Appendix F: Scope, Exclusions, and Use of This Document 110
F.1 Purpose and Scope 110
F.2 What This Report Does 110
F.3 What This Report Does Not Do 111
F.4 Treatment of Evidence and Uncertainty 111
F.5 Use and Citation of This Document 111
F.6 Relationship to Other Assessments 111
F.7 Closing Statement 112
Appendix G: Experimental Seepage Erosion and Channelisation Framework (after Berhanu et al., 2012) 113
Appendix H - Contextual Spatial Overlay: Independent Subsurface Reference Geometry and LiDAR Elevation Change 117
Appendix I - Table of Figures 118

1. Introduction

1.1 Purpose of submission

This document presents a structured record of observed bank erosion, seepage, and associated surface and near-surface hydrological features identified at multiple locations within the study area. The purpose of the submission is to document these observations in a consistent, spatially referenced manner and to present them for regulatory consideration within the remit of watercourse management, bank stability, and groundwater-surface water interaction.

The purpose is to support determination of whether the observed features warrant further site inspection, monitoring, or review under existing regulatory powers.

1.2 Scope of the report

The scope of this report is limited to observable physical features and spatial patterns relevant to:

- bank stability and erosion along watercourses,
- seepage and groundwater emergence at bank faces,
- sediment mobilisation and deposition within channels, and
- the relationship between these features and broader landscape-scale elevation change.

Evidence is drawn from a combination of aerial imagery, LiDAR elevation differencing (2018-2022), and ground-based observations recorded between 2018 and January 2026. Each location is presented individually using a consistent structure to allow comparison across sites.

This report does not assess operational compliance, subsurface engineering integrity, or chemical water quality exceedances, except insofar as surface observations intersect with watercourse behaviour and temporal persistence beyond individual rainfall events.

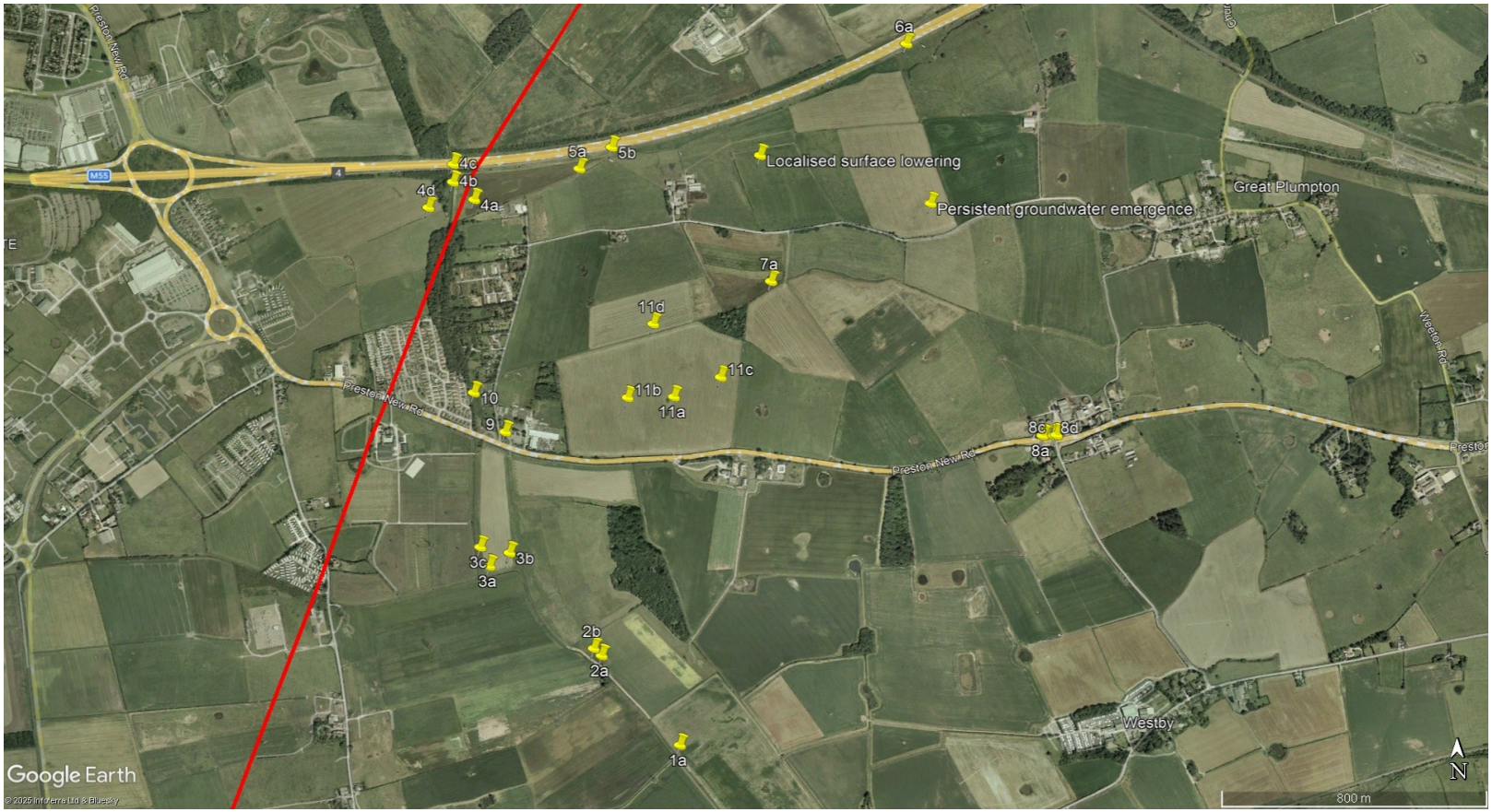

Figure 1 - Regional context of study area prior to 2011.

Overview of the areas presented in this report, shown using Google Earth imagery dated January 2005. Yellow pins indicate the approximate locations of surface features and field areas examined in subsequent sections, rather than specific image acquisition points.

The red line indicates the approximate surface projection of a fault in the Wakepark area as described by Smythe (2020). It is included for geographic and contextual reference only and is not used as a basis for spatial attribution or interpretation elsewhere in the report.

This figure provides pre-2011 baseline context for landscape form and drainage prior to subsequent changes documented in later figures.

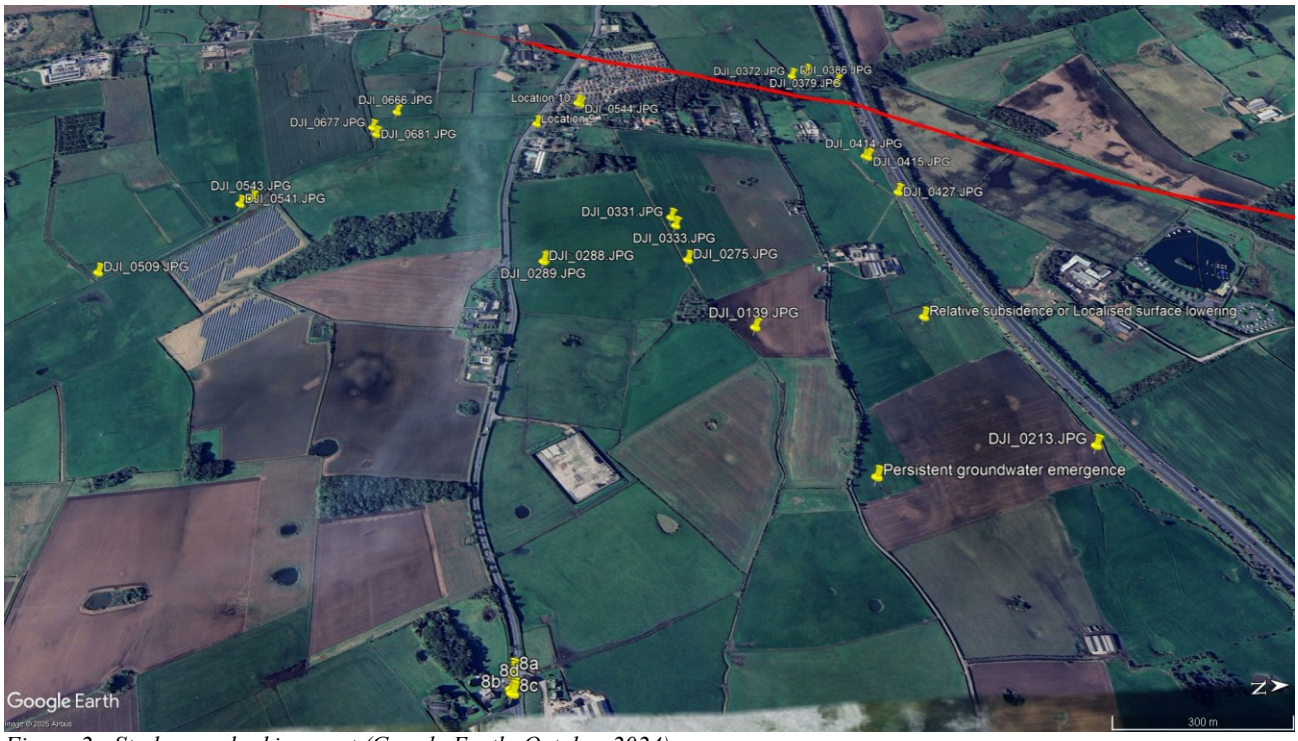

Figure 2 - Study area looking west (Google Earth, October 2024)

Oblique Google Earth view of the study area looking west, showing the relationship between fields, drainage channels and watercourses across the wider landscape. This view provides spatial context for the locations presented in this report and illustrates the low-relief, drainage-dependent nature of the setting. Pins with ".JPG" in the title represent UAV positions at the time of image capture, as recorded in Appendix A.

1.3 Explicit exclusions and evidential limits

This submission does not seek to establish causation, attribute responsibility, or infer specific subsurface mechanisms. No conclusions are drawn regarding the origin, depth, or driving processes underlying the observed features.

The emphasis throughout is on what is directly observable, spatially coherent, and temporally persistent. Interpretative statements are limited to describing scale, geometry, and recurrence, with the objective of enabling informed regulatory judgement rather than asserting impact.

2. Methods and data sources

2.1 Overview

This report is based on the systematic review and comparison of spatial and photographic data from multiple sources selected to document observable bank erosion, seepage, and associated surface features in relation to surrounding landform and watercourse behaviour. The approach prioritises repeatability, spatial reference, and consistency across locations.

Each location is presented using the same sequence of datasets to allow direct comparison and to distinguish persistent features from transient or isolated effects.

2.2 Aerial and satellite imagery

High-resolution satellite imagery from Google Earth was used to provide landscape-scale context for each location. Time-stamped imagery was reviewed to identify the persistence, expansion, or migration of wet ground, standing water, and surface disturbance over time.

Google Earth imagery is used solely for contextual and comparative purposes, including identification of spatial patterns and temporal continuity. No measurements or elevation values are derived from satellite imagery.

2.3 LiDAR elevation differencing (2018-2022)

LiDAR data from 2018 and 2022 were processed and differenced to identify relative elevation change over the four-year period. The resulting rasters were examined for spatial coherence, scale, and alignment with observable surface features.

LiDAR elevation change is used in this report to characterise the spatial extent and distribution of relative elevation variation. It is not used to infer causation, depth of change, or specific subsurface processes. Throughout this section, interpretation is limited to the presence, continuity, and geometry of relative elevation differences; LiDAR is therefore used solely to establish spatial continuity and persistence of surface expression, not magnitude, rate, or mechanism of change.

For clarity and consistency, LiDAR elevation change figures include an inner bounding box delineating the specific observation location and an outer bounding box showing the spatial extent of the immediately preceding contextual figure. This framing is used solely for orientation and does not alter the underlying raster data.

2.4 Aerial photography (28/01/2026)

Aerial imagery acquired on 28 January 2026 was used to document current site conditions at each location. These images provide intermediate-scale resolution between satellite imagery and ground photography, enabling visual assessment of bank morphology, channel condition, field wetness, and surface disturbance.

Aerial imagery refers to UAV-acquired images used in the following Locations. Ground-based imagery is used at selected locations (including Locations 4 and 8-10) where access was available.

Some localised colour features (e.g. red/orange staining at bank emergence points) are more clearly resolved in RAW (DNG) imagery than in compressed JPEG exports used for document figures; where relevant, this is noted, and original RAW and JPEG versions are retained in the image archive (where DNG capture was enabled on the UAV.)

2.5 Ground-based photography (2018-2026)

Ground photographs taken between 2018 & 2026 were used to document bank face condition, seepage points, sediment staining, iridescence, and material loss where accessible. These images are used to show detail not visible in aerial datasets and to confirm features identified remotely. Ground photography is treated as observational evidence of surface condition only and is not used to infer subsurface structure or processes.

2.6 Location structure and presentation

Twelve locations are presented in this report. For each location, the following sequence is used unless otherwise stated:

- Google Earth overview for spatial context
- LiDAR elevation change raster (2018-2022)
- Aerial or ground-based imagery
- Zoomed detail or additional contextual imagery where required

This consistent structure is intended to make similarities and differences between locations readily apparent and to support regulatory review.

This report does not seek determination of cause. It seeks recognition that the documented features are persistent, spatially clustered, and directly interact with watercourses, and that existing monitoring arrangements are not designed to resolve their origin or significance. On that basis, it is reasonable to request further assessment within the Agency's remit for water quality protection and bank stability, without pre-empting conclusions on subsurface mechanisms that sit beyond the scope of this document.

2.7 Consistency of Figure Selection and Presentation

The number, type, and scale of figures presented for each location vary according to the complexity and evolution of observable surface features at that site. Locations exhibiting stable or singular expressions are documented using fewer figures, while locations showing temporal change, spatial migration, or multiple interacting surface expressions are supported by additional imagery to adequately characterise observed behaviour.

Where multiple figures are presented in sequence, this reflects the need to document change over time, differences in water level or surface condition, or the relationship between broad context and fine-scale features. In such cases, wider-context images are paired with intermediate or close-range views to clarify interpretation and to distinguish active surface expressions from static or superficial features such as vegetation, debris, or legacy disturbance.

Figure numbering follows document order rather than geographic hierarchy. Where additional figures are inserted during iterative review to improve clarity or completeness, numbering is adjusted accordingly to maintain sequential consistency. The inclusion of additional figures does not imply increased severity or impact at a given location, but reflects the need for clear visual documentation of observable conditions.

All figures are presented for descriptive purposes only. No inference is made regarding causation, subsurface pathways, or mechanism beyond what is directly observable in the imagery.

3. Study area overview

3.1 - Geographic and hydrological setting

The study area comprises low-lying agricultural land intersected by a network of drainage channels and watercourses. Land use is predominantly pastoral, with fields bounded by drainage ditches, minor watercourses, and access tracks. Ground elevations are shallowly graded, and surface water management relies heavily on open channels and bank integrity to maintain drainage function.

Watercourses within the study area form part of an interconnected drainage system, with banks that are locally steepened, artificial in places, and sensitive to changes in water level, seepage, and

material strength. Small variations in bank condition or near-surface or shallow subsurface water movement can therefore have disproportionate effects on erosion, channel stability, and sediment delivery.

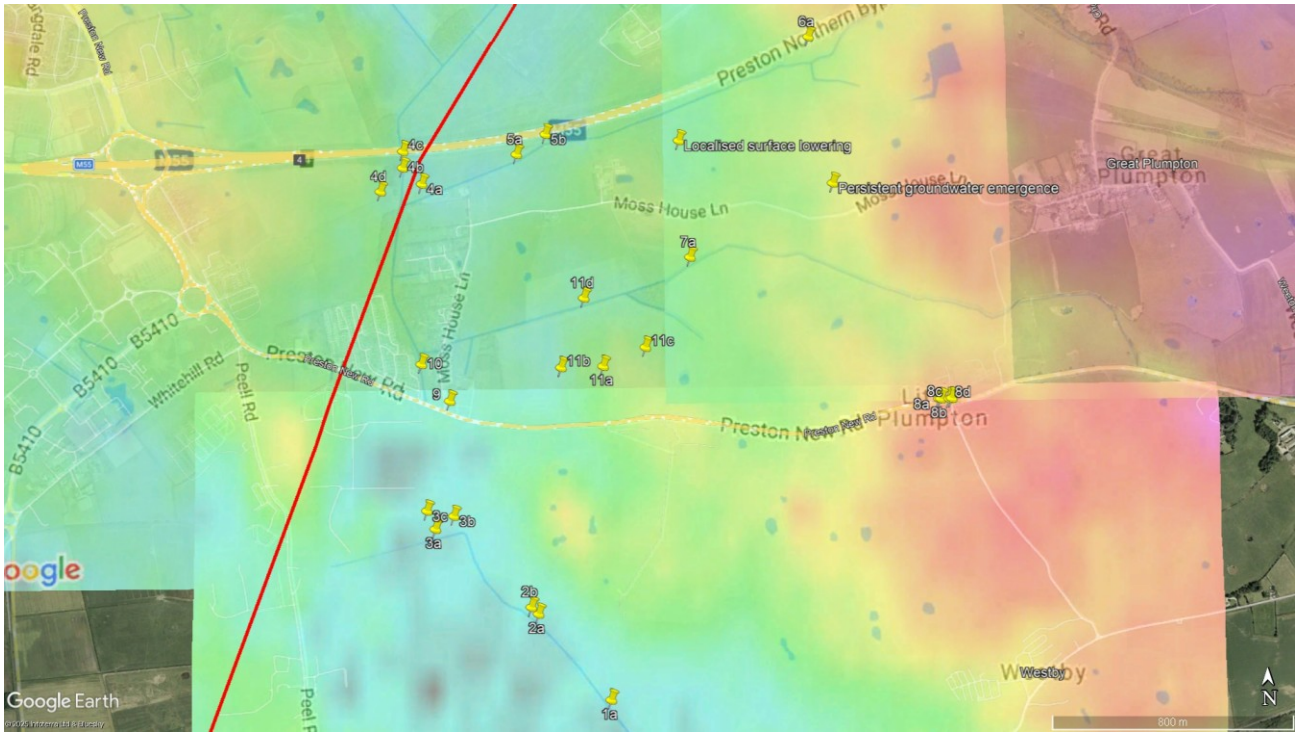

Figure 3 - Broad topographic context of the study area (historical elevation data)

Topographic context generated from historical digital elevation data projected into Google Earth Pro in 2018. Exact processing dates are unavailable; however, the underlying elevation datasets pre-date the surface expressions described in this report. The figure is used qualitatively to illustrate broad-scale spatial relationships, gradients, and low-lying zones across the study area, rather than to derive quantitative measurements.

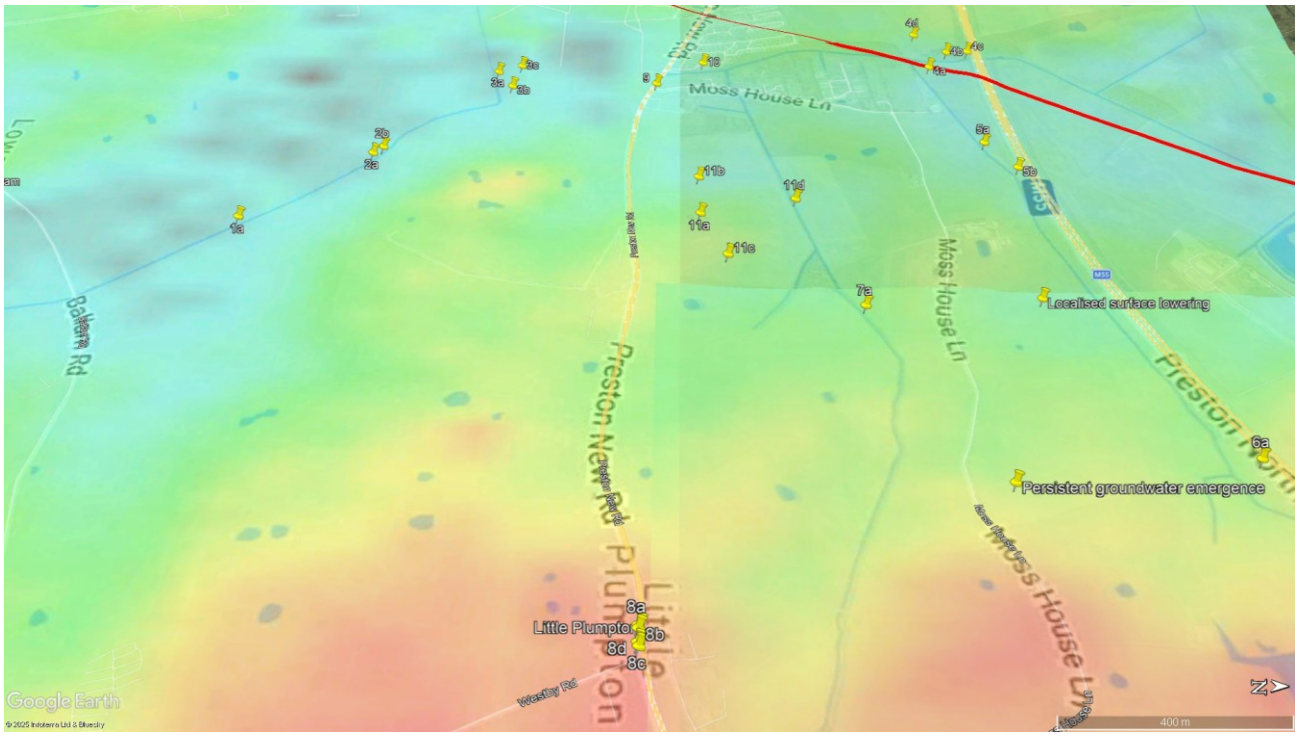

Figure 4 - Topographic context looking west.

Oblique view of the same historical topographic surface shown in Figure 3, viewed looking west. This perspective illustrates the shallow relief of the landscape and the continuity of low-gradient transitions between fields, drainage features, and watercourses across the study area.

3.2 - Surface water behaviour and bank sensitivity

Across the study area, standing water, seasonally wet ground, and persistent ponding are recurrent features in multiple fields. These surface expressions are not confined to individual parcels but occur across contiguous areas, often in proximity to watercourses or drainage lines.

Bank stability in this setting is influenced not only by channel flow but also by groundwater emergence, soil saturation, and fine sediment mobilisation. Where seepage occurs at or near the bank face, erosion can be accelerated through undercutting and loss of cohesion, even in the absence of high-flow events.

3.3 - Relevance to the locations presented

The locations documented in this report were selected because they exhibit visible interactions between land surface condition and adjacent watercourses, including erosion, seepage, staining, or material loss. In several cases, these localised features occur within broader zones of persistent wet ground or elevation change identified through remote sensing and elevation context imagery.

The purpose of presenting multiple locations within a single study area is to allow comparison of form, scale, and recurrence, and to assess whether observed bank erosion and seepage represent isolated incidents or components of a wider pattern affecting watercourse stability.

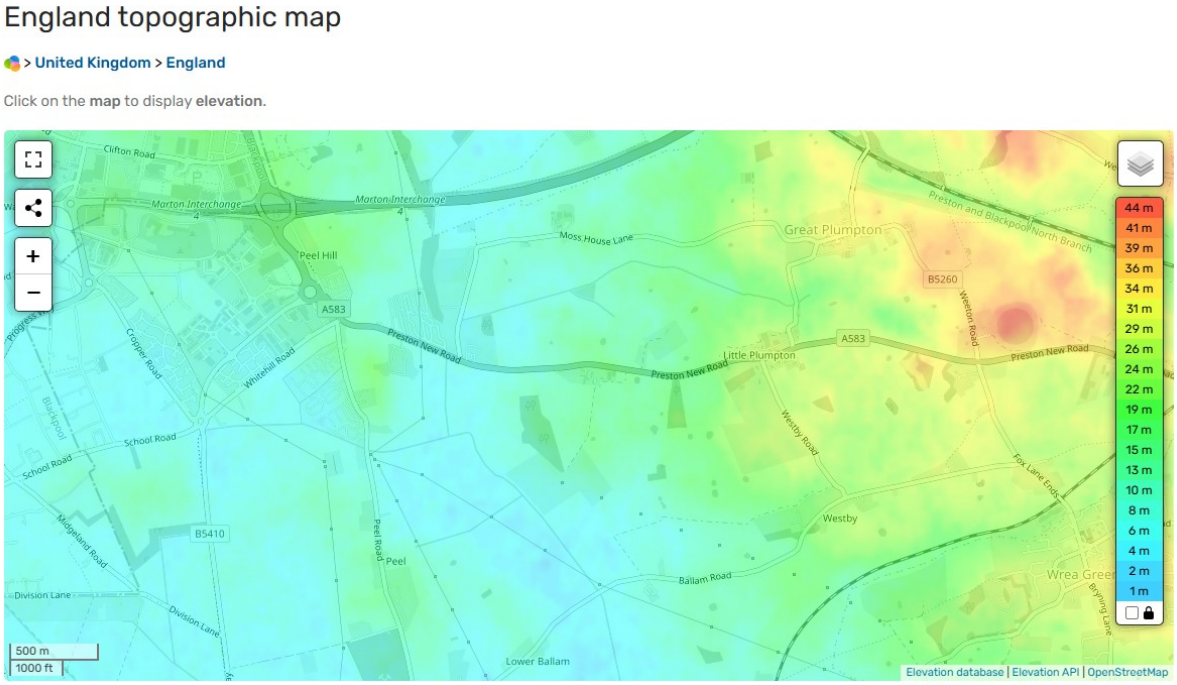

Figure 5 - Contemporary topographic projection and persistent low-gradient geometry (accessed 2026)

Accessed in 2026 (topographic-map.com, derived from public elevation datasets) showing a persistent low-gradient elevation transition across the study area. The geometry corresponds spatially with areas of repeated surface wetness, standing water, and bank sensitivity documented elsewhere in this report, and provides additional contextual confirmation of the landscape-scale setting in which the observed features occur.

Against this low-relief, drainage-dependent topographic setting, the following sections document site-specific observations of bank erosion, seepage, and surface water behaviour at selected

locations across the study area. Each location is presented individually using a consistent structure, allowing observed features to be considered both in their immediate context and in relation to the wider landscape conditions described above.

4. Locations Overview of Location Framework and Reference Infrastructure

The following section documents field observations, aerial imagery, and remote sensing evidence from discrete identified locations within the study area. Each location has been selected based on observable surface expression, geomorphic change, or hydrological connection. For clarity and consistency, all spatial references in this section are provided relative to a common infrastructural and topographic framework described below.

Preston New Road Well Pad

The Preston New Road well pad ("the pad") serves as a fixed spatial reference point throughout Section 4. The pad is located immediately south of the M55 motorway corridor within an agricultural, low-lying landscape dissected by surface watercourses, field drains, and land drainage features. Where distances or directional references are used, they relate to the pad perimeter unless otherwise specified.

Main Drain and Catchment Setting

The wider study area lies within the Main Drain and Ribble Valley catchment. The Main Drain is a formally designated channel that receives flow from smaller watercourses, including Carr Bridge Brook, and conveys surface water in a generally north-south direction toward the River Ribble estuary at Lytham St Annes. The Carr Bridge Brook, situated to the north of the pad, flows into the Main Drain system approximately 1.2 km to the west of the pad location, and is part of the broader land drainage network within which the pad and associated observation points are situated. The interaction of these drainage features with the local topography and groundwater pathways forms an important contextual backdrop to the locations described herein.

4.1 Location 1

Location 1 is situated to the south of Preston New Road and to the north of Ballam Road, adjacent to the Main Drain. The surrounding land is low-lying and agricultural, with drainage reliant on a combination of buried piping, open channels, and bank integrity.

This location is included because it exhibits visible bank erosion, seepage, and persistent wet ground in proximity to the watercourse, occurring within a broader area of landscape-scale elevation change identified through LiDAR analysis. The site provides a clear example of how field-scale conditions intersect with channel margins.

Figure 6 shows the immediate landscape context of Location 1, including the relationship between the affected bank section, adjacent fields, and local drainage features.

Figure 6 - Location 1: Site context and surrounding landscape (Google Earth image, 06/24)

Google Earth image showing Location 1 within its immediate landscape context. The image illustrates the proximity of the affected bank section to the adjacent watercourse, surrounding fields, and drainage features. Areas of exposed or disturbed bank material and localised wet ground are visible along the channel margin. Green polygon outlines the approximate view shown in Figure 8.

Figure 7 presents LiDAR elevation differencing for Location 1, used to place the observed bank features within their wider field-scale elevation context.

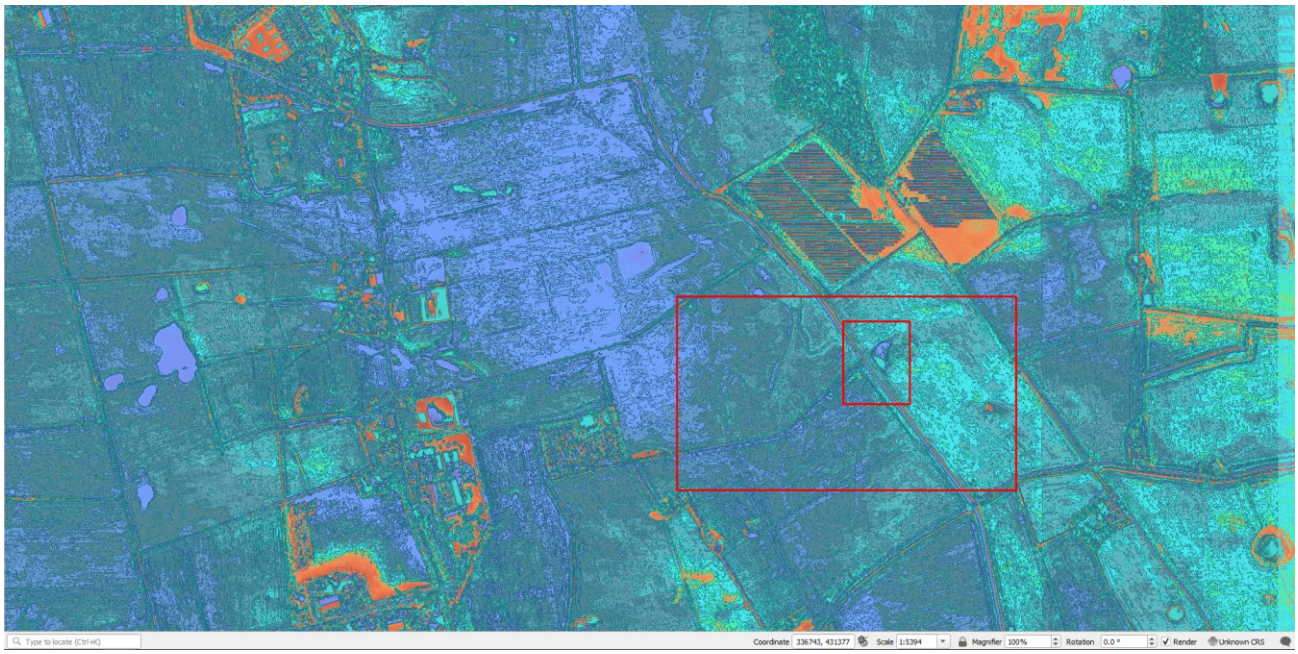

Figure 7 - Location 1: LiDAR elevation change context (2018-2022)

LiDAR elevation differencing between 2018 and 2022 for Location 1, showing areas of relative elevation loss and gain across the surrounding landscape. Zones of elevation decrease extend beyond the immediate watercourse and bank margins into adjacent fields, forming spatially coherent, field-scale patterns rather than isolated, discontinuous features. The extent and continuity of these changes are not confined to surface drainage lines or parcel boundaries, indicating spatially coherent elevation change across the landscape over the period assessed.

The elevation changes shown in Figure 7 occur across a broader area than the immediate watercourse and include contiguous zones of relative elevation loss extending into adjacent fields. Within this wider setting, erosion and seepage observed along the bank provide a visible surface expression of interaction at the interface between land and channel. The following figures document how these broader field-scale changes manifests locally, where groundwater emergence, material loss, and water-sediment interaction are directly observable.

Figure 8 - Location 1a Bank morphology and adjacent field context (28/01/2026)

Aerial view of the watercourse bank at Location 1 showing erosion along the channel margin in the context of surrounding fields exhibiting persistent wet ground and standing water. The bank displays undercutting and localised material loss, forming a narrow zone where changes observed at field scale intersect with the watercourse. This interface represents a point at which subsurface or near-surface water movement becomes externally visible. (Approx. UAV centre: 53.777335 N, -2.961047 W facing East-North-East)

Figure 9 - Location 1a: Detail of seepage, staining, and surface water characteristics.

Close-up view of seepage emerging from the bank face at Location a1, with associated orange sediment staining along the waterline. The staining is spatially localised at discrete emergence points rather than uniformly distributed along the bank, and coincides with zones of active erosion and fine sediment deposition within the channel.

4.1.1 - Summary of observations (Location 1)

LiDAR elevation differencing between 2018 and 2022 shows spatially coherent zones of elevation loss extending across multiple adjacent fields at Location 1, rather than being confined to the immediate watercourse or bank margin. These changes form contiguous patterns that do not align with field boundaries, drainage infrastructure, or isolated surface features.

Within this wider area of elevation change, erosion and seepage are observed along the bank of the adjacent watercourse. The bank exhibits undercutting, material loss, and discrete points of groundwater emergence, providing a visible surface expression at the land-channel interface. Red/orange sediment staining and localised surface iridescence are present at these emergence points and coincide with active erosion and fine sediment deposition in the channel.

Taken together, the observations at Location 1 indicate that bank instability and seepage occur within a broader zone of landscape-scale elevation change, and that the bank represents a focal point where subsurface or near-surface water movement becomes externally observable. These features are therefore best considered as part of a connected system rather than as isolated or purely localised bank processes.

4.2 - Location 2

Location 2 is situated approximately 400 m northwest of Location 1, along the same watercourse corridor. The surrounding land is similarly low-lying and agricultural, with drainage reliant on buried field piping, open channels, and bank integrity.

This location is included because it exhibits bank instability and seepage features comparable in form to those observed at Location 1, and lies adjacent to an area of persistent field wetness to the west that has previously exhibited ponding in the absence of recent rainfall.

Figure 10 shows the immediate landscape context of Location 2 and the position from which ground-based imagery was acquired.

Figure 10 - Location 2: Site context and image positions (Google Earth, June 2024)

Google Earth view of Location 2 showing the relationship between the watercourse, adjacent fields, and the area of recurrent surface wetness located to the west of the channel. Image positions for DJI_0541.DNG and DJI_0543.JPG are indicated to provide spatial reference for the ground-based observations presented below.

Figure 11 presents LiDAR elevation differencing for Location 2, used to place the observed bank features and adjacent field conditions within their wider field-scale elevation context.

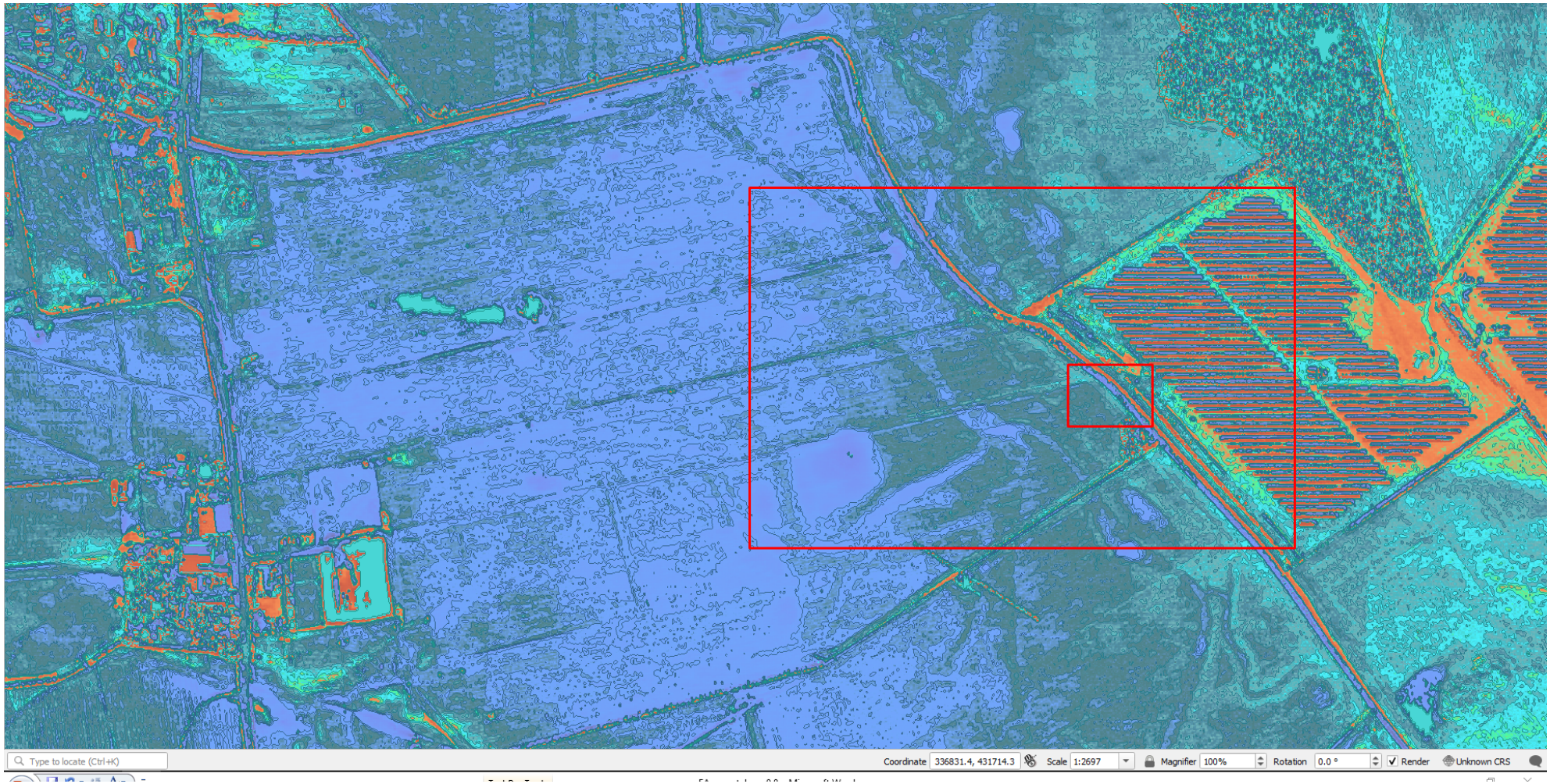

Figure 11 - Location 2: LiDAR elevation change context (2018-2022)

Showing spatially coherent zones of relative elevation change across adjacent fields and along the watercourse corridor. Areas of elevation loss extend beyond the immediate channel margin and are expressed at field scale, forming contiguous patterns that do not align with parcel boundaries or drainage infrastructure. The distribution of these changes overlaps with areas of recurrent surface wetness observed to the west of the channel.

Figure 12 - Location 2A: Aerial image showing bank condition and channel context (28/01/2026)

Aerial image showing the watercourse bank at Location 2, with visible undercutting and localised material loss along the channel margin. The bank face displays discrete zones of erosion rather than continuous uniform retreat, and the adjacent channel shows fine sediment accumulation at the waterline. Vegetation cover above the bank is discontinuous, with exposed soil visible in places along the bank face. (Approx. UAV centre: 53.779886 N, -2.964604 W facing East-North-East)

Figure 13 - Location 2A: Aerial zoomed view of bank erosion and seepage at the waterline (28/01/2026)

Zoomed view derived from aerial imagery at Location 2 highlighting discrete seepage points, undercutting, and associated sediment staining along the channel margin.

Figure 14 - Location 2B: Aerial image facing northwest along the watercourse (28/01/2026)

Aerial image facing northwest along the watercourse at Location 2, showing continued bank erosion and areas of red/orange staining along the channel margin. The staining is visible at discrete sections of the bank and corresponds approximately with the mapped image position of DJI_0543 shown in Figure 10. Water within the channel appears more turbid adjacent to the affected bank sections than in upstream reaches. (Approx. UAV centre: 53.779886 N, -2.964604 W facing North-West)

Figure 15 - Zoomed view derived from ground-based imagery at Location 2.

Focusing on the bank face and adjacent waterline, localised seepage and bank erosion are visible, together with a distinct change in water colour and increased turbidity in the immediate vicinity of the bank.

4.2.1 Summary of observations (Location 2)

LiDAR elevation differencing between 2018 and 2022 shows spatially coherent zones of relative elevation change at Location 2, extending across adjacent fields and along the watercourse corridor. These changes are expressed at field scale and are not confined to the immediate channel margin, forming contiguous patterns that do not align with parcel boundaries or drainage infrastructure. Areas of elevation change overlap with zones of recurrent surface wetness observed to the west of the watercourse.

Within this broader field-scale setting, aerial imagery documents bank erosion and seepage at discrete locations along the channel margin. The bank exhibits localised undercutting and material loss, with erosion occurring at specific points rather than as uniform retreat along the bank. These features are visible at multiple positions along a short reach of the same drainage corridor.

At Location 2, changes in water appearance are observed adjacent to affected bank sections, including increased turbidity in the immediate vicinity of seepage and erosion points. Taken together, the observations indicate that bank instability and altered water characteristics at Location 2 occur within a wider zone of landscape-scale elevation change and persistent wet ground, and are not isolated to a single point along the watercourse.

4.3 Location 3

Location 3 is situated on the north bank of The Main Drain, a primary drainage channel along an approximately east-west oriented reach, directly south of the junction of Preston New Road and Moss House Lane. The watercourse here forms part of the primary drainage network within the study area and is bordered by intensively managed agricultural land.

This location was selected because it provides a clear and relatively recent aerial record of surface change along the bank and adjacent field margin. The imagery shows visible surface disturbance, localised vegetation stress, and changes in ground condition that have developed over time along a well-defined section of the drainage corridor. The site also allows comparison between surface expressions observed in aerial imagery and broader elevation patterns identified through LiDAR analysis.

Figure 16 presents a Google Earth overview of Location 3, showing the position of the bank section within the wider landscape and drainage network.

Figure 16 - Location 3: Aerial overview of bank and adjacent field condition. (Google Earth; 10/2024)

Aerial image showing the north bank of the main drainage channel at Location 3. The image highlights surface disturbance along the bank margin and adjacent field, including areas of uneven ground texture and patches of vegetation stress. These features are spatially concentrated along the channel corridor rather than uniformly distributed across the surrounding fields, and are visible along a continuous reach of the bank.

Following initial drafting, a further bank feature was identified within the same reach during continued imagery review and is documented here as DJI_0666.

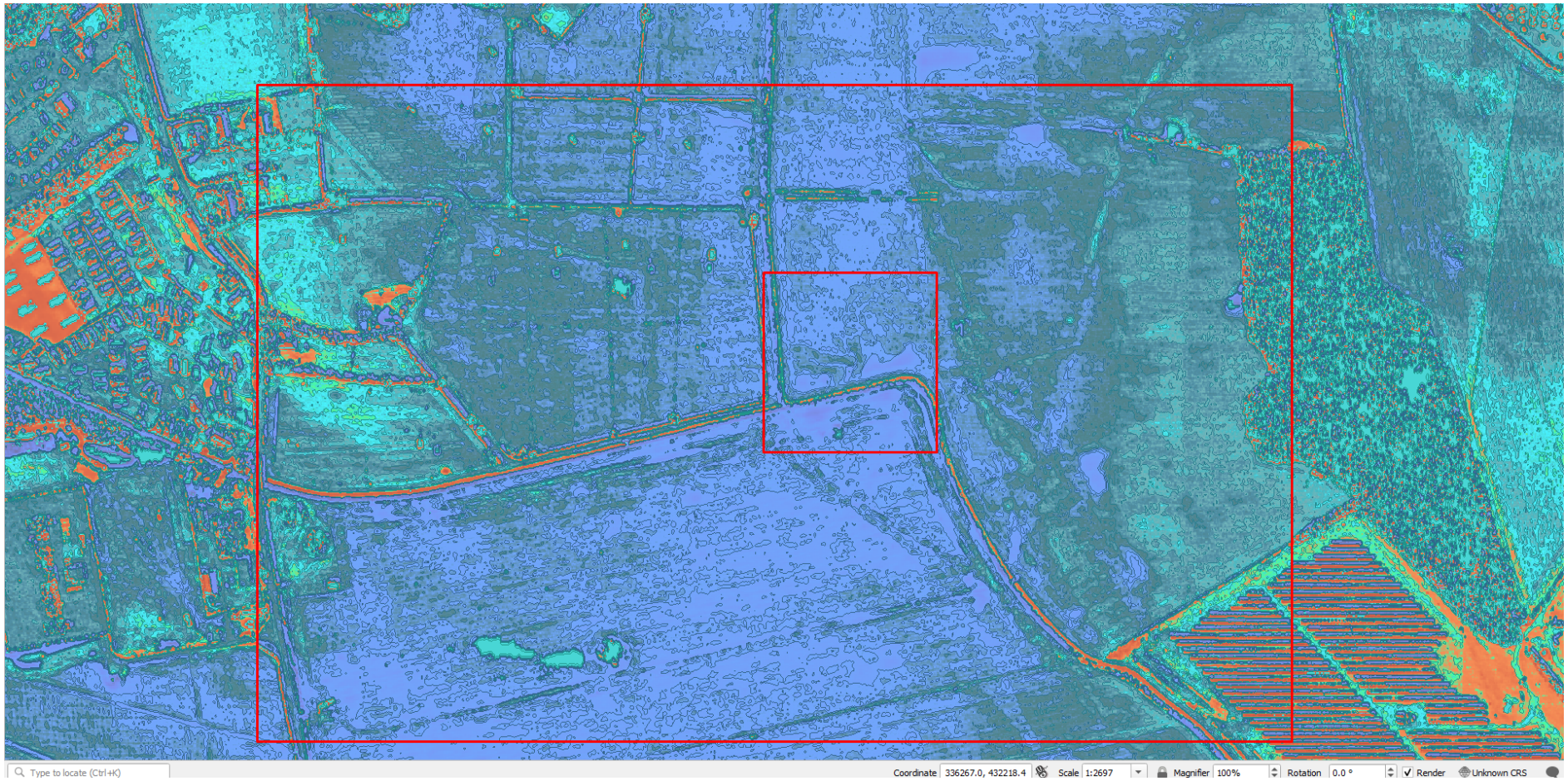

Figure 17 - Location 3: LiDAR elevation change context (2018-2022)

LiDAR elevation differencing between 2018 and 2022 for Location 3, showing spatially coherent zones of relative elevation change across the fields adjoining the main drain. Areas of elevation loss extend along and beyond the channel corridor, forming elongated patterns that are not confined to field boundaries or surface drainage features. The distribution of these changes provides field-scale context for the surface disturbance and vegetation stress observed along the bank in Figure 16.

The following figures document localised bank disturbance at Location 3, including discrete bank-face openings and associated waterline staining.

Figure 18 - Location 3A: Aerial image showing bank condition and localised bank-face opening (28/01/2026)

Aerial image of the north bank of the main drain at Location 3 showing localised bank instability. A discrete, narrow opening is visible at the top of the bank face, with adjacent bank edge irregularity and localised material loss along the channel margin. The bank profile in the vicinity of the opening is uneven compared to adjacent sections, suggesting a point feature rather than uniform retreat along the reach. (Approx. UAV centre: 53.782503 N, -2.969205 W facing North)

Figure 19 - Location 3A: Aerial zoomed view derived from above UAV RAW imagery.

Showing a discrete opening at the top of the bank face and associated bank edge irregularity. The opening exposes darker internal material within the bank and is aligned with a narrow zone of disturbance at the waterline. In the RAW (DNG) imagery, localised red/orange staining is visible at the base of the feature; this staining is not consistently reproduced in compressed JPEG exports used for document presentation and is noted here for transparency.

Figure 20 - Location 3B: Aerial image showing bank-face opening with associated staining at the waterline (28/01/2026)

Aerial image showing a discrete opening at the top of the north bank at Location 3B, with exposed internal bank material and a narrow zone of red/orange staining extending from the bank face to the waterline. The staining is spatially confined to the vicinity of the opening and coincides with localised bank disturbance and fine sediment accumulation within the channel. (Approx. UAV centre: 53.782618 N, -2.968746 W facing North)

Figure 21 - Zoomed aerial view showing the bank-face opening and associated red/orange staining at the waterline at Location 3B.

A section of broken or exposed drainage pipe is visible in the adjacent field upslope of the bank, within the immediate vicinity of the bank disturbance. The pipe is noted here as a local landscape feature; no functional connection is inferred.

Location 3C is situated northeast of Locations 3A and 3B along the east bank of the north-south oriented reach of the Main Drain. The location was included following identification of an additional discrete seepage feature exhibiting visible staining and bank disturbance, spatially separated from previously documented features but occurring along the same channel reach.

Figure 22 - Location 3C: Site context and spatial relationship (aerial image 28/01/2026)

Aerial view showing the position of Location 3C along the east bank of the north-south oriented section of the Main Drain, northeast of Locations 3A and 3B. The image provides spatial context, illustrating the relative separation between observed seepage points and their alignment along the same bank reach. Image pin labels indicate the approximate locations of aerial observations referenced in Figures 23 and preceding figures. (Approx. UAV centre: 53.783021 N, -2.970237 W facing North)

Figure 23 - Location 3C: Bank seepage and erosion detail (aerial image)

Zoomed aerial view of the east bank at Location 3C showing a discrete seepage point emerging from the bank face. A narrow linear zone of red/orange staining extends downslope from the emergence point to the channel margin, coincident with localised bank erosion and fine sediment disturbance. The staining is spatially confined and contrasts with adjacent bank sections where no comparable discharge is visible.

4.3.1 Summary of observations (Location 3)

Observations at Location 3 comprise multiple discrete seepage and erosion features (Locations 3A, 3B, and 3C) distributed along the east bank of the Main Drain across both east-west and north-south oriented channel sections. These features are spatially separated but occur along the same continuous bank reach.

Across all sub-locations, erosion and seepage are characterised by localised bank undercutting, fine sediment disturbance, and discrete emergence points rather than uniform degradation along the channel margin. At several points, narrow linear zones of red/orange staining extend downslope from bank-face emergence points to the waterline, indicating focused discharge pathways rather than diffuse surface runoff.

LiDAR elevation differencing for the surrounding area indicates field-scale elevation change extending beyond the immediate channel margins. Within this wider context, the bank features observed at Location 3 represent surface expressions occurring where subsurface or near-surface water movement intersects the channel boundary. The recurrence of similar bank-scale features at multiple, non-contiguous points along the same reach suggest a connected setting rather than isolated local failures.

Taken together, the observations at Location 3 demonstrate that bank instability and seepage are repeated phenomena along this section of the Main Drain, occurring within a broader landscape-scale setting and manifesting at discrete points where channel banks provide an outlet for water and sediment movement.

4.3.2 Closing Statement – Locations 1–3 (Lower and Mid-Corridor Observations)

Locations 1-3 document a series of surface and near-surface features occurring primarily within agricultural land and along drainage-channel margins in the vicinity of Preston New Road. Across these locations, recurring observations include bank erosion, seepage, sediment staining, persistent wet ground, fines mobilisation, and localised surface deformation*.

** term used as surface expression only.*

Although the features vary in form and intensity between locations, they display consistent alignment with drainage corridors and low-gradient ground, and persist across multiple observation periods. In several cases, surface expressions extend beyond immediate channel margins into adjacent fields, indicating that observed processes are not confined solely to open watercourses. LiDAR elevation differencing and aerial imagery provide corroborative context, demonstrating that these surface features occur within broader zones of subtle but coherent ground change rather than as isolated disturbances.

Taken together, Locations 1-3 establish the baseline pattern of ground and hydrological sensitivity within the study area. They demonstrate that surface response is already present within agricultural and drainage-channel settings prior to the later expressions observed in infrastructure-adjacent and residential contexts. These early locations therefore provide essential context for understanding how similar processes manifest across different land uses and degrees of engineering control elsewhere in the study area.

4.4 Location 4

Location 4 is situated south of the M55 at the point where the Main Drain passes beneath the motorway corridor. The location comprises a small cluster of aerial and ground observations focused on the west side of the channel immediately downstream of the motorway crossing. The site captures a transition zone where surface drainage, agricultural land use, and subsurface structure intersect, and where disturbance features are expressed across both banks and adjacent fields.

Figure 24 - Site overview and image orientation (Google Earth, 06/2024)

Provides spatial context for Location 4. The image shows a cluster of three aerial image pins defining the location, with an additional pin indicating a single ground-based photograph included for completeness. The green polygon denotes the approximate viewing footprint of image DJI_0379, illustrating camera orientation and coverage relative to the Main Drain, the motorway corridor, and surrounding fields.

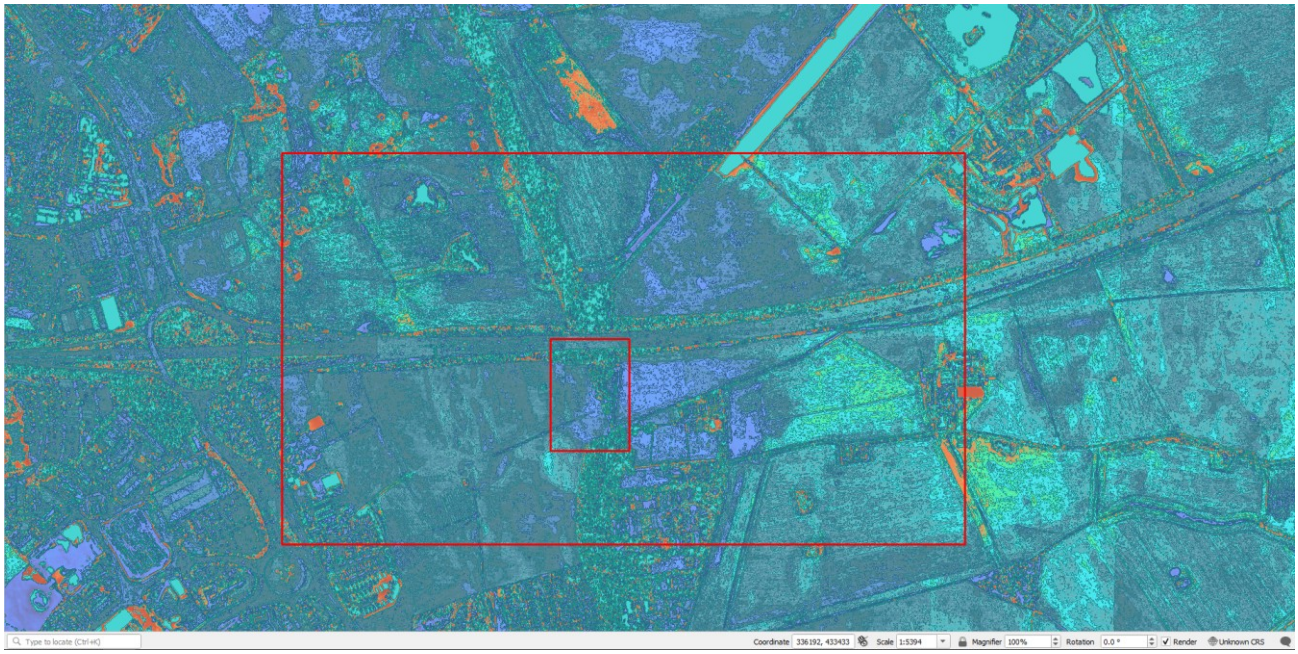

Figure 25 - Location 4: LiDAR elevation change context (2018-2022)

LiDAR elevation differencing between 2018 and 2022 for Location 4, showing a continuous zone of relative low elevation extending beneath and beyond the M55 corridor. The cluster of observations comprising Location 4 lies on the western margin of this low-lying area. The elevation change pattern is spatially coherent at field scale and extends across mapped linear features, including projected fault traces, rather than being confined to the immediate channel margins or surface infrastructure.

Figure 26 - Location 4a, overview and surface context (22/10/2018)

Oblique aerial view showing Location 4 south of the M55 where the Main Drain passes beneath the motorway. The image illustrates the broader field context, including subtle linear surface mounding and discontinuities running parallel to the watercourse and to a tributary of the Main Drain. The position of the ground reference image (Figure 28) is indicated in Figure 27 for spatial context. (Approx. UAV centre: 53.793053 N, -2.972114 W facing East-North-East)

Figure 27 - Magnified view of the same area, identifying the position of the ground-based photograph presented in Figure 28.

The fence line adjacent to the drain is visibly non-linear, with curvature and offset inconsistent with normal installation tolerances. Ground disturbance adjacent to the fence mirrors deformation patterns observed on the opposite bank, reinforcing the interpretation that these features are not confined to a single landholding or drainage asset.

Figure 28 - Ground-level surface disturbance at Location 4 (22/10/2018)

Ground photograph corresponding to the location indicated in Figure 27, showing a localised surface scarp and adjacent disturbed ground. The feature includes a steepened break in slope and lobate, fine-grained material at its base, morphologically resembling a small scarp with associated mud-rich extrusion. (Approx centre: 53.79338 N, -2.971416 W facing North-North-West)

While temporally earlier than the aerial imagery presented elsewhere in this section, the ground photograph documents a deformation style consistent with later surface expressions observed nearby and is included here to illustrate the form and scale of disturbance present within the same drainage setting. In the top right of Figure 28 the motorway bridge over the Main Drain can be seen, presented in Figure 29

Figure 29 - Aerial image (28/01/2026) of the southern section of the M55 culvert at the Main Drain crossing.

The image shows the motorway embankment and adjacent agricultural fields. Linear surface repairs and areas of resurfacing are visible on the carriageway, while neighbouring fields exhibit irregular surface texture and localised wetness consistent with ground stress in the vicinity of the drainage corridor. (Approx. UAV centre: 53.793752 N, -2.971375 W facing North)

Figure 30 - Magnified aerial view of the motorway bridge embankment at the Main Drain crossing.

Detail view showing a localised protrusion of sediment into the watercourse from the western edge of the embankment, indicating focused material delivery at the bank-structure interface.

Figure 31 - Aerial view of ground depressions SSE of the motorway bridge.

Aerial image showing a cluster of discrete circular to sub-circular ground depressions located south-southeast of the motorway bridge and slightly upslope from previously documented bank and culvert-related features. The depressions are distributed across pasture and do not align with visible drainage infrastructure or field management patterns. (Approx. UAV centre: 53.792673 N, -2.971925 W facing North-North-East)

Figure 32 - Zoomed aerial view showing fluid-filled depressions and fence-line continuity.

Magnified view of the depressions shown in Figure 31. Several features contain dark to reddish-coloured standing water. The depressions extend across a fence line, indicating they are not confined to a single grazing unit or caused by localised livestock activity.

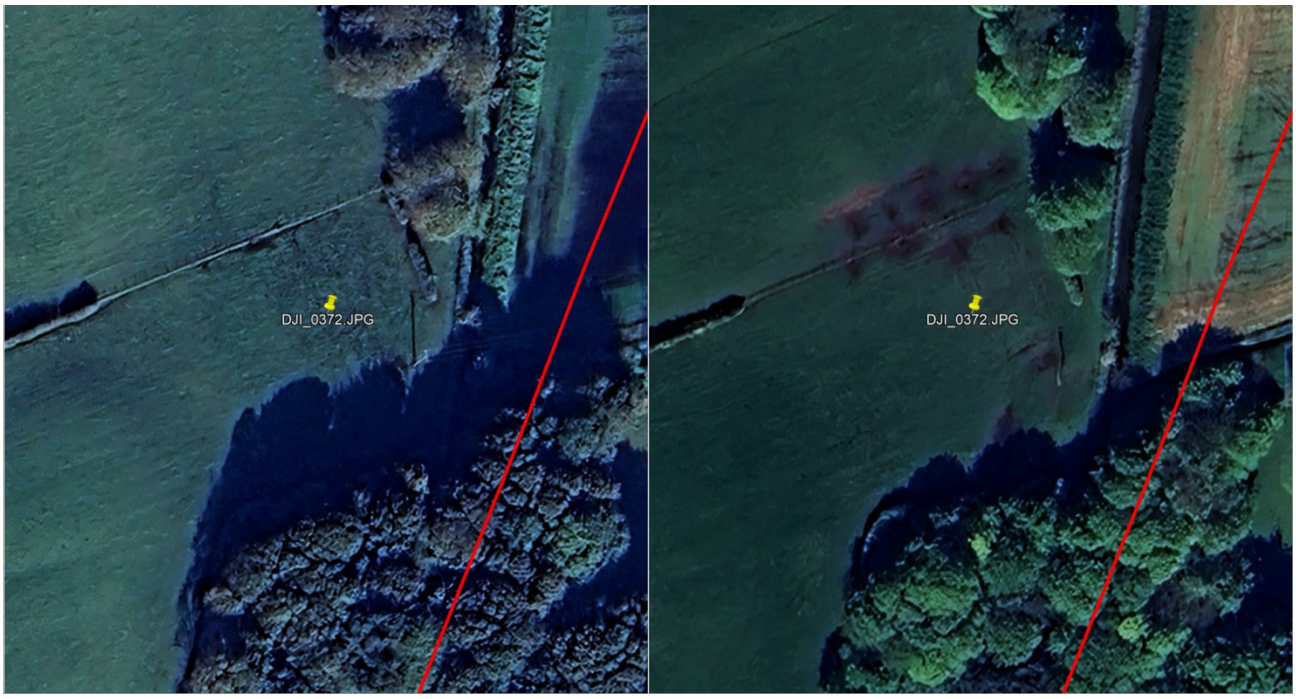

Figure 33 - Temporal comparison of ground condition prior to and following depression formation.

Side-by-side Google Earth imagery showing the same location in October 2024 (left) and May 2025 (right). In October 2024 the ground exhibits irregular surface patterning and tonal variation at the same location, prior to the appearance of the circular depressions visible in May 2025. This comparison indicates that anomalous ground conditions were present before the formation of the discrete circular features.

4.4.1 - Summary of observations (Location 4)

Observations at Location 4 document a convergence of surface deformation, anomalous ponding, and sediment mobilisation in the immediate vicinity of a major drainage structure beneath the M55 corridor. Features include localised scarps and mud-rich surface disturbance, deformation of fence alignments adjacent to the channel, sediment protrusion at the embankment-bank interface, and the emergence of discrete circular depressions upslope of the watercourse.

LiDAR differencing indicates that these features are situated along the margin of a spatially coherent low-elevation zone that extends beneath the motorway corridor and across mapped linear structures, rather than being confined to the immediate channel banks. Temporal comparison shows that anomalous ground conditions were present prior to the appearance of discrete depressions, suggesting progressive surface expression rather than abrupt localised failure.

Taken together, the observations at Location 4 indicate sustained ground sensitivity within a drainage-dependent setting, where surface deformation, seepage, and sediment redistribution recur across multiple years and across both sides of the channel. No causal mechanism is assigned at this stage; however, the consistency of form, alignment, and temporal development warrants consideration of Location 4 as part of a wider pattern addressed in subsequent locations.

4.5 - Location 5

Location 5 lies immediately east of Location 4 along the southern side of the M55 corridor, adjacent to a tributary of the Main Drain visible in DJI_0379. The location comprises two aerial observations positioned within an agricultural field south of the motorway, selected due to the presence of linear surface disturbance and vegetation stress aligned with drainage and subsurface structural trends identified elsewhere in the study area.

Figure 34 - Location 5: Aerial overview (May 2025)

Top-down aerial image showing Location 5, situated east of Location 4 along the M55 corridor. Two image pins define the location. A crack-like linear surface pattern is visible within the field south of the motorway, accompanied by zones of vegetation stress. These features occur across areas with differing land cover, including cropped and uncropped ground.

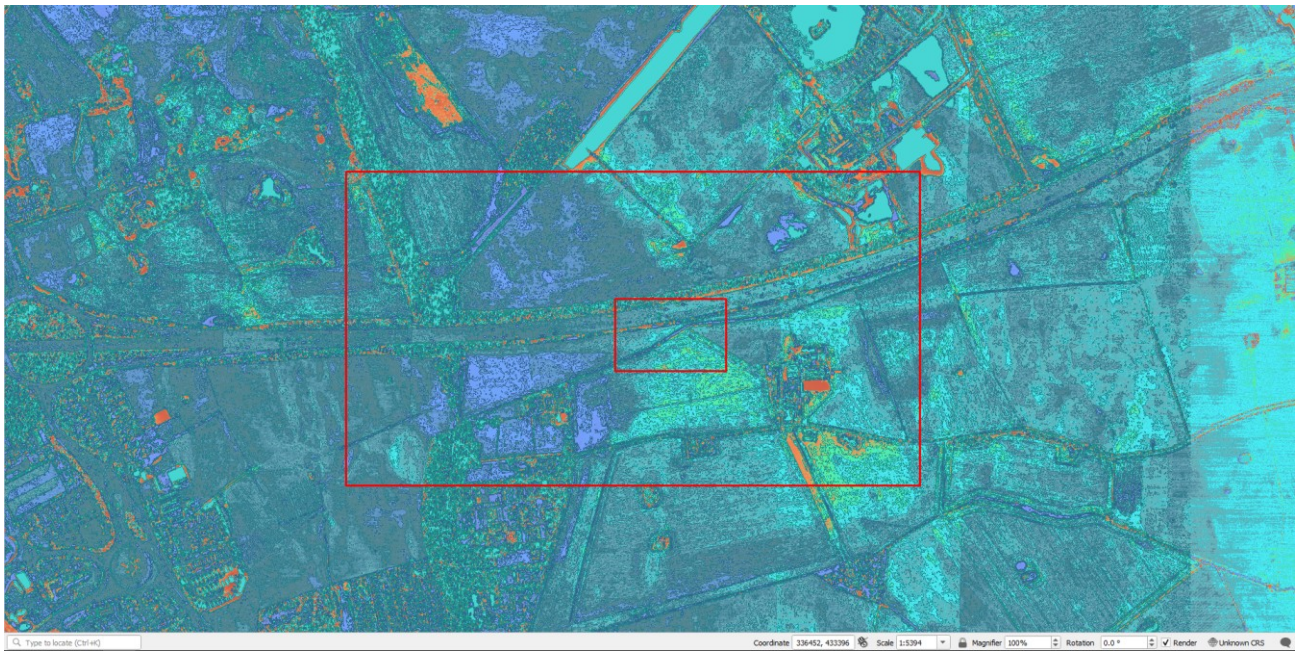

Figure 35 - Location 5: LiDAR elevation change context (2018-2022)

LiDAR elevation differencing for the Location 5 area. Geometric elevation patterns correspond spatially with surface expressions visible in aerial imagery, including linear features and zones of anomalous surface condition extending across field boundaries and towards the adjacent drainage corridor.

Figure 36 - Location 5a, Aerial view of linear surface features adjacent to tributary

Oblique aerial image showing linear surface patterns and low mounded features extending across the field toward the tributary channel. Subtle tonal variation and surface texture changes are visible along these alignments. A telegraph pole within the field is visibly leaning to the North. Localised disturbance to the channel bank is visible in the lower right of the image. (Approx. UAV centre: 53.793979 N, -2.966135 W facing East-South-East)

Figure 37 - Location 5a, Localised bank disturbance at tributary (DJI_0414)

Closer aerial view of the bank disturbance identified in Figure 36, captured in a separate image (DJI_0414). The channel margin shows irregular geometry and disturbed vegetation. Low mounded features are visible on the opposite side of the channel, indicating similar surface expressions on both banks. (Approx. UAV centre: 53.793917 N, -2.966213 W facing South-South-East)

Figure 38 - Location 5a, Detail view of surface features and infrastructure deformation (DJI_0414)

Closer of the area shown in Figure 36, focusing on the leaning telegraph pole and adjacent surface features. Shallow ponding, low mounds, and areas of darker staining are visible in proximity to the linear surface patterns extending toward the tributary. A thin surface film or scum is visible along the margin of one sediment-stained area, marking a distinct boundary between standing water and surrounding ground.

Figure 39 - Location 5b: ponding and bank-adjacent staining near the motorway corridor.

Aerial view showing persistent ponding close to the motorway embankment, with reddish staining visible on the opposite bank of the watercourse. A fan-shaped zone of disturbed ground extends downslope from the stained area in the adjacent field. Low mounds and irregular surface texture are present within and around this zone, correlating spatially with field-scale disturbances documented elsewhere in the study area. (Approx. UAV centre: 53.794415 N, -2.963893 W facing North-East)

4.5.1 Summary of observations (Location 5)

Observations at Location 5 document linear surface disturbance, anomalous ponding, and vegetation stress within an agricultural field adjacent to a tributary of the Main Drain along the southern margin of the M55 corridor. Surface expressions include crack-like linear features, low mounded ground, shallow ponding, and localised bank disturbance, occurring on both sides of the tributary channel.

LiDAR elevation differencing provides contextual evidence that these surface features lie within a broader zone of spatially coherent elevation change extending across field boundaries and toward the drainage corridor. The alignment of linear surface features, infrastructure deformation (including a leaning telegraph pole), and bank-adjacent disturbance suggests that ground response at Location 5 is not confined to a single point or asset.

Taken together, the observations at Location 5 indicate ongoing interaction between surface water behaviour, ground condition, and drainage infrastructure within a low-relief, drainage-dependent setting. No causal mechanism is inferred; however, the consistency of surface form and spatial

alignment supports consideration of Location 5 as part of the wider pattern of ground sensitivity documented across the study area.

4.6 - Location 6

Location 6 is located approximately 900 m east-north-east of Location 5b (Figure 39) and spans the M55 motorway corridor. The location captures surface expressions that extend across agricultural land on both sides of the motorway and intersect with the broader drainage network.

Figure 40 - Location 6: Aerial overview and image orientation (28/01/2026)

Aerial image showing Location 6, with the green polygon indicating the viewing footprint and orientation of the image. Surface expressions visible in Google Earth imagery from April 2020 include irregular linear and patchy zones of tonal variation within fields adjacent to the motorway. These features persist across field boundaries and are not aligned with visible agricultural operations or drainage infrastructure.

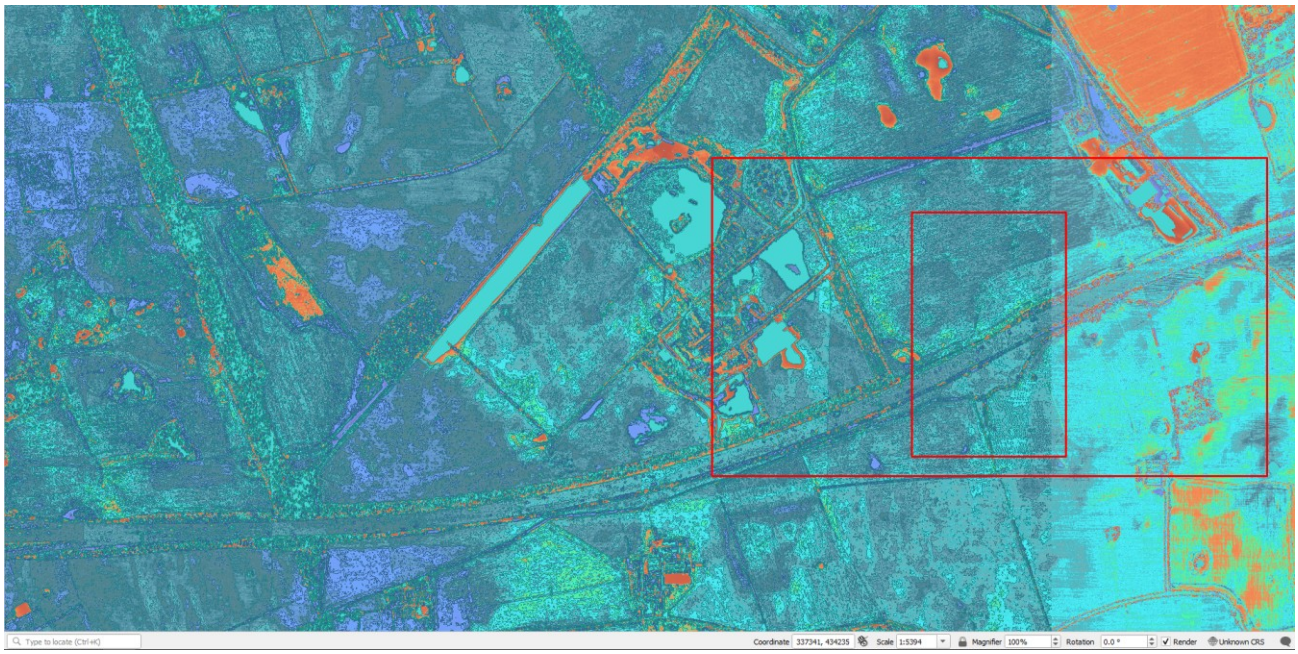

Figure 41 - Location 6: LiDAR elevation change context (2018-2022)

LiDAR elevation differencing for Location 6 shows spatially coherent elevation changes extending across the motorway corridor and into adjacent fields. The pattern is not confined to embankments or cuttings and intersects mapped linear features.

Together, the aerial and elevation datasets indicate that surface anomalies at Location 6 form part of a continuous zone of ground sensitivity that crosses infrastructure boundaries and persists over multiple years. As with preceding locations, observations are presented descriptively, without attribution of cause, to support comparison with other sites within the study area.

Figure 42 - Aerial view of Location 6a facing northeast (28/01/2026)

Aerial image showing Location 6 spanning the M55 corridor. To the north of the motorway, linear cracking and tonal variation are visible within the field, consistent with shallow surface disturbance and preferential moisture pathways. To the south of the motorway, discrete surface mounds and irregular ground texture are present within pasture adjacent to the drainage network, indicating deformation expressed on both sides of the infrastructure corridor. (Approx. UAV centre: 53.796556 N, -2.951206 W facing North-East)

4.6.1 Summary of observations (Location 6)

Location 6 documents surface disturbance expressed across a broad corridor intersected by the M55, including cracking, seepage-related tonal variation, and low-amplitude mounding. Features are present both north and south of the motorway and extend across agricultural land, drainage features, and the transport corridor itself.

Elevation variation is expressed across multiple surface types and land uses, extending beyond individual field parcels and engineered features. Instead, they are consistent with shallow ground response and differential settlement influenced by subsurface hydrological or structural controls acting at field-to-corridor scale.

No causal interpretation is assigned at this stage; however, the recurrence of similar surface expressions across multiple locations strengthens the case that Location 6 forms part of a wider pattern of ground sensitivity associated with the drainage corridor and underlying ground conditions.

4.6.2 Section Summary - Locations 4 to 6

Locations 4, 5, and 6 collectively document a sequence of surface deformation features distributed along and across the M55 corridor, including scarps, mounds, circular depressions, seepage staining, cracking, and subtle elevation change. These features recur across multiple land parcels, cross fence lines and infrastructure boundaries, and are expressed both upslope and downslope of drainage channels.

LiDAR differencing indicates that several of these surface expressions coincide with broader zones of elevation change, suggesting landscape-scale controls rather than isolated failures. Temporal imagery shows that anomalous ground conditions often precede the formation of discrete features, indicating progressive rather than instantaneous development.

Taken together, these locations demonstrate consistent deformation styles expressed across different surface contexts within the same drainage and infrastructure setting. While causal mechanisms are not assigned here, the observations provide a coherent basis for considering subsurface hydrological connectivity, ground sensitivity, and cumulative infrastructure interaction in subsequent sections.

4.7 Location 7

Location 7 is situated approximately 450 m north-west of the Preston New Road pad perimeter, on the southern bank of Carr Bridge Brook. The brook runs broadly east-west across a sequence of agricultural fields and represents a downstream drainage element that is distinct from, but hydrologically connected to, the Main Drain system. This location is representative of several reaches along Carr Bridge Brook where similar bank-related disturbances and adjacent field surface anomalies are observed.

Figure 43 - Overview of Location 7 and surface context (Google Earth, 08/2025)

Top-down aerial view showing Location 7 on the southern bank of Carr Bridge Brook. The image highlights irregular surface patterning within the field adjacent to the watercourse, including diffuse tonal variation and subtle linear surface features extending away from the bank. These patterns are not aligned with cultivation rows or field boundaries and are spatially associated with the course of the brook. Localised bank irregularities and vegetation discontinuities are visible along the channel margin, indicating areas of bank stress or material loss.

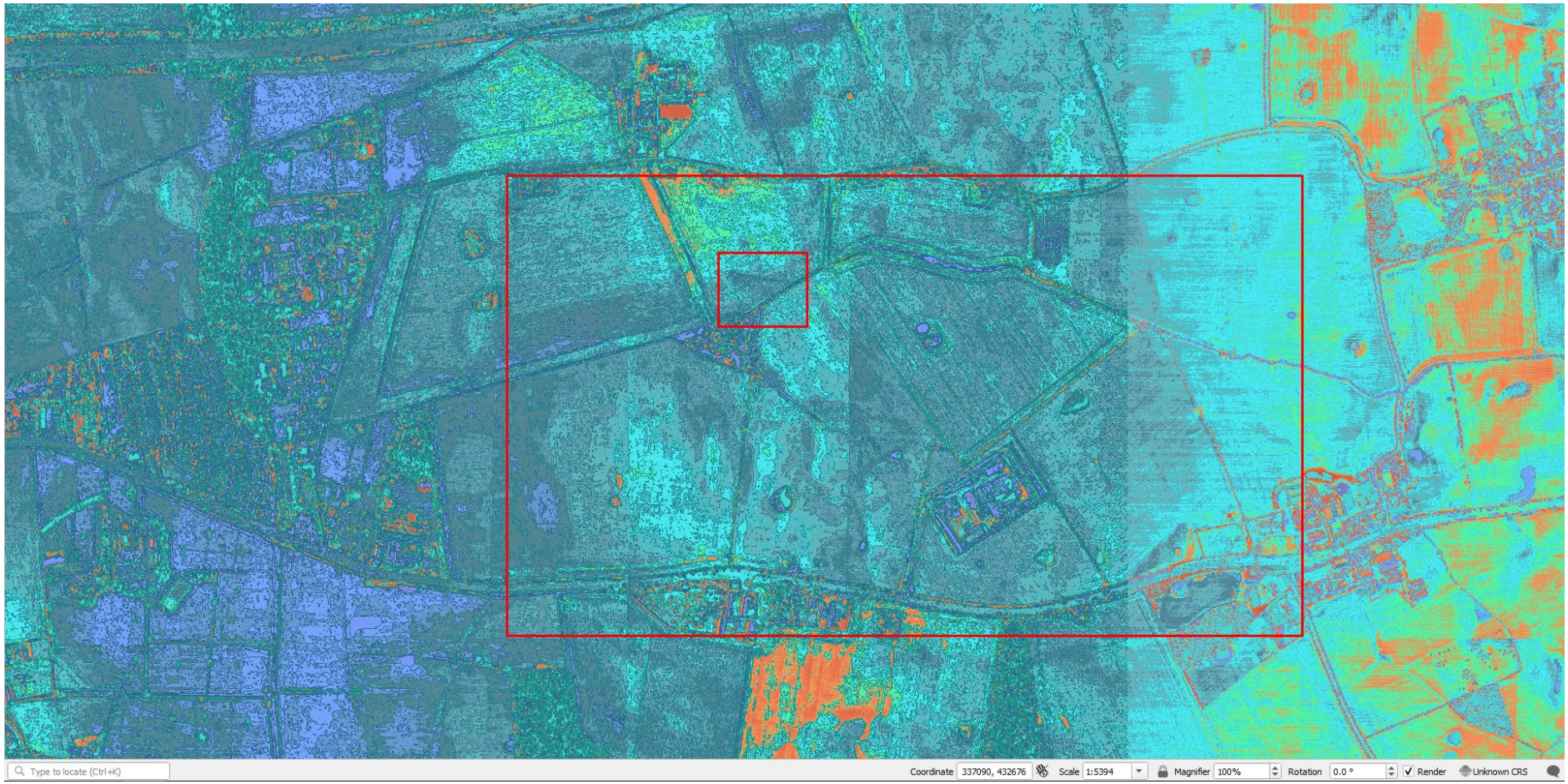

Figure 44 - Location 7: LiDAR elevation change context (2018-2022)

LiDAR elevation differencing for Location 7 showing field-scale geometry consistent with the surface expressions visible in Figure 43. Zones of relative elevation change extend along the southern bank of Carr Bridge Brook and into the adjacent field, rather than being confined to the immediate channel edge. The spatial coherence of these changes follows the brook alignment and persists across field boundaries, indicating a repeated pattern of ground response along this reach of the watercourse.

Figure 45 - Location 7: Bank erosion and channel-margin instability along CBB.

Oblique aerial image showing a section of the CBB channel with pronounced bank undercutting, exposed soil faces, and localised collapse of the channel margin. The erosion is laterally continuous along the bank and coincides with a narrow zone of disturbed ground extending into the adjacent field. The fence has visibly fallen from the bank, indicating loss of lateral support rather than progressive wear or livestock interaction. The geometry and extent of material loss are inconsistent with routine maintenance or isolated livestock damage and indicate ongoing bank instability driven by active hydrological and ground-response processes. (Approx. UAV centre: 53.790768 N, -2.956884 W facing South-East)

4.7.1 Interim Synthesis and Summary - Locations 1-7

Across Locations 1-7, a consistent set of surface expressions has been documented within a shared low-lying, drainage-dependent landscape. These include bank erosion, seepage, sediment staining, surface cracking, circular depressions, linear mounding, fence deformation, and persistent wet ground. While individual features vary in form and scale, they recur within a coherent spatial framework defined by drainage corridors, shallow gradients, and mapped or inferred subsurface structure.

Remote sensing (Google Earth time series and LiDAR differencing) demonstrates that many of these features evolve over time, with anomalous surface conditions often preceding the appearance of more discrete disturbances such as depressions, scarps, or focused erosion. Several features are observable on both sides of field boundaries, fence lines, and drainage assets, indicating that their origin is not confined to local land management practices or isolated infrastructure failures.

These patterns are consistent with preferential subsurface flow, progressive weakening, or piping-type processes acting within a hydraulically sensitive setting. Importantly, the observations are not restricted to channel margins but occur upslope and at distance from visible surface drainage, suggesting broader subsurface connectivity.

No single causal mechanism is asserted at this stage. However, taken collectively, the observations demonstrate that the study area exhibits systemic ground sensitivity, with surface water behaviour and erosion responding to factors beyond normal seasonal variation. The recurrence, geometry, and temporal development of the features documented here indicate that these are not isolated incidents, but components of a wider pattern affecting watercourse stability and adjacent land.

The following sections build on this foundation by examining additional locations and considering the implications of these observations for infrastructure integrity, drainage performance, and long-term ground stability.

4.7.2 - Intervening Field between Locations 6 and 7

These fields lie between Locations 6 and 7, approximately midway along the southern side of the M55 corridor. Although no mapped surface watercourse crosses the fields, they occupy the same broader topographic and structural corridor identified in adjacent locations.

Figure 46 - Intervening fields between Locations 6 and 7 (Google Earth, 04/2025).

Top-down Google Earth imagery showing two adjacent fields situated between Locations 6 and 7 along the southern side of the M55 corridor. The fields exhibit patchy surface disturbance, tonal variation, and irregular ground texture not aligned with field boundaries or agricultural practices.

A point of localised surface lowering identified in LiDAR elevation differencing (2018-2022), is indicated within the western field. Additional features include a mapped area of persistent groundwater emergence along Moss House Lane and areas of persistent wetness and staining within the fields.

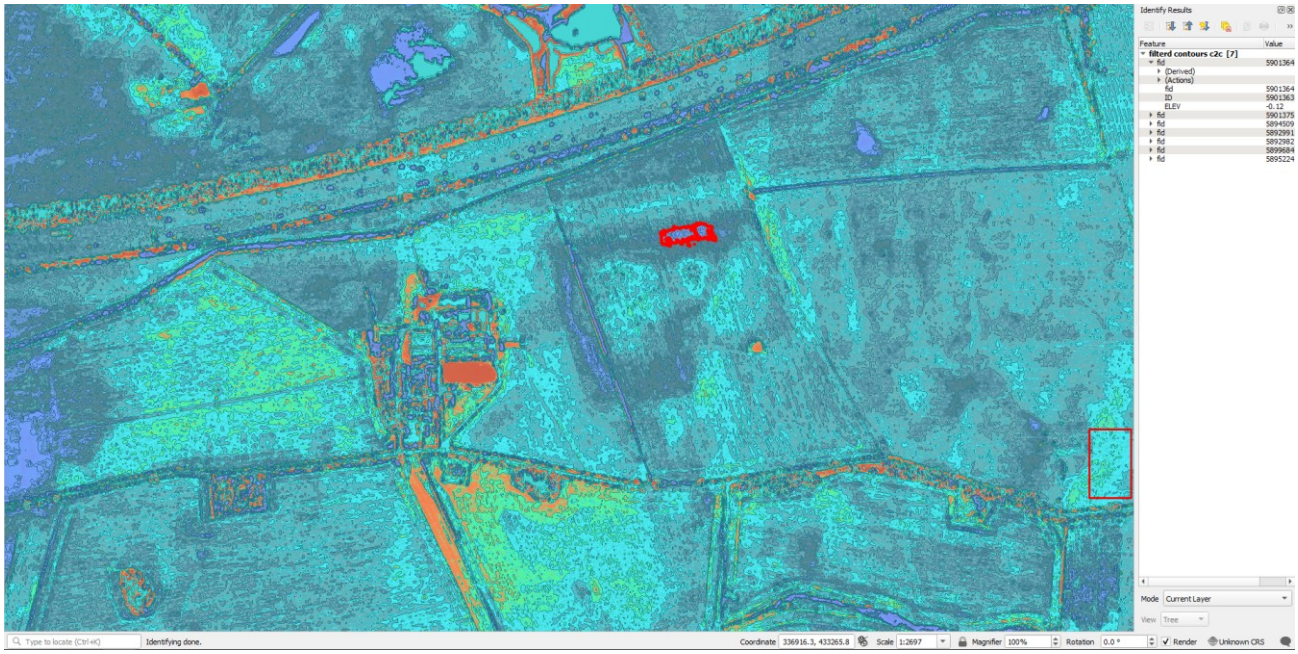

Figure 47 - Bridging fields between Locations 6 and 7: LiDAR elevation change context (2018-2022)

Contour projection derived from LiDAR elevation differencing, filtered to emphasise low-magnitude change. A localised closed depression of approximately 0.12 m is evident within the field area between Locations 6 and 7, spatially coincident with surface disturbance and seepage features observed in aerial imagery. The geometry is discrete, persistent, and not aligned with field boundaries or agricultural operations, supporting its interpretation as a real surface deformation rather than an artefact of land use or data processing.

Although no formal watercourse crosses these fields, their position and surface expression provide a spatial link between deformation observed north of the pad, at the motorway corridor, and along downstream locations, supporting interpretation of field-scale continuity of ground disturbance across the area.

Historical Google Earth imagery (April 2025) shows tonal and surface irregularities within the field, while oblique aerial imagery from 28/01/2026 documents more clearly expressed surface disturbance and localised seepage. LiDAR elevation differencing (2018-2022) indicates up to ~12 cm of relative surface lowering within the same area.

Figure 48 - Oblique aerial view of intervening fields prior to observed deformation (24/08/2017).

Oblique aerial image showing the intervening fields between Locations 6 and 7 prior to the development of surface disturbance documented in later imagery. The field surface appears laterally uniform, with continuous cultivation patterns and no evidence of localised subsidence, ponding, seepage, or irregular tonal variation. The motorway corridor and adjacent fields corresponding to Location 6 are visible in the same frame, providing spatial continuity across the study area. This image establishes a pre-disturbance baseline against which subsequent surface deformation and LiDAR-detected elevation change can be compared

Figure 49 - Oblique aerial view of ground deformation within an intervening field between Locations 6 and 7 (28/01/2026).

Oblique aerial image showing a zone of irregular surface expression characterised by shallow depressions, patchy ponding, and diffuse surface staining that cross-cut cultivation marks. The deformation exhibits a gently curvilinear surface geometry and subtle tonal contrasts consistent with differential ground moisture and surface lowering rather than alignment with agricultural activity. This field lies between Locations 6 and 7 and corresponds spatially with a localised area of LiDAR-detected elevation loss (~0.12 m between 2018-2022), providing field-scale context for the distributed nature of surface deformation across this sector. Approx. UAV centre: 53.794165 N, -2.957151 W facing North-East)

Notably, areas of red and locally iridescent surface films associated with seepage are present in close proximity to the deformation, despite the absence of formal drainage infrastructure. The field therefore provides an important spatial link between deformation observed north of the pad, at the motorway corridor, and along watercourses downstream.

Figure 50 - Persistent groundwater staining in bridging fields between Locations 6 and 7.

Aerial image showing a narrow, branching seepage feature expressed as pale, reflective flow paths with adjacent reddish-brown staining and localised ponding. The seepage follows a sinuous, downslope trajectory that cross-cuts cultivation marks, indicating control by subsurface pathways rather than surface agricultural activity. The seepage occurs ~450 m south of Location 6 and ~500 m southeast of the subsidence feature identified in the adjacent field, while that subsidence lies ~380 m north of Location 7. Although spatially separated, these features fall within the same broader zone of LiDAR-detected elevation change (~0.12 m between 2018-2022), suggesting distributed ground response rather than isolated surface effects. (Approx. UAV centre: 53.792479 N, -2.950323 W facing East-North-East)

While this location is not associated with a defined watercourse, its inclusion here is warranted as it demonstrates continuity of ground disturbance across multiple land parcels and reinforces the interpretation that observed deformation is not confined to channelised flow paths.

4.7.3 Summary of observations (Location 7)

The observations documented at Location 7 and within the intervening fields between Locations 6 and 7 reinforce the presence of distributed ground disturbance across the southern side of the M55 corridor. Although these fields are not intersected by a formal watercourse, their surface behaviour mirrors that observed along adjacent drainage features, including Carr Bridge Brook and upstream locations closer to the pad.

The combination of historical aerial imagery, recent oblique surveys, and LiDAR elevation differencing demonstrates that surface deformation within this area is both spatially coherent and temporally progressive. Features such as localised subsidence, diffuse seepage, persistent wet

ground, and irregular surface patterning were not present in earlier imagery but have developed over time within a shared topographic and structural corridor.

Importantly, these features are not constrained by field boundaries, land use, or surface drainage infrastructure. Instead, they extend across multiple parcels and occur both upslope and downslope of established watercourses, suggesting that the observed ground response reflects broader subsurface controls rather than isolated surface processes.

The intervening fields therefore provide a critical spatial and interpretive link between deformation observed north of the pad, within the motorway corridor, and downstream along Carr Bridge Brook. Their inclusion strengthens the interpretation that ground disturbance within the study area is distributed, connected, and not limited to channelised flow paths.

The following section builds on this evidence by examining additional locations and considering the implications of these observations for infrastructure stability, drainage performance, and longer-term ground behaviour across the wider area.

4.8 Location 8

Location 8 is situated approximately 400 m east-south-east of the pad, on the southern side of Preston New Road (A583) at Little Plumpton. The location occupies a grassed embankment and pedestrian verge immediately south of the carriageway and outside a formal surface watercourse, but within the same broader low-lying drainage and infrastructure corridor identified elsewhere in the study area.

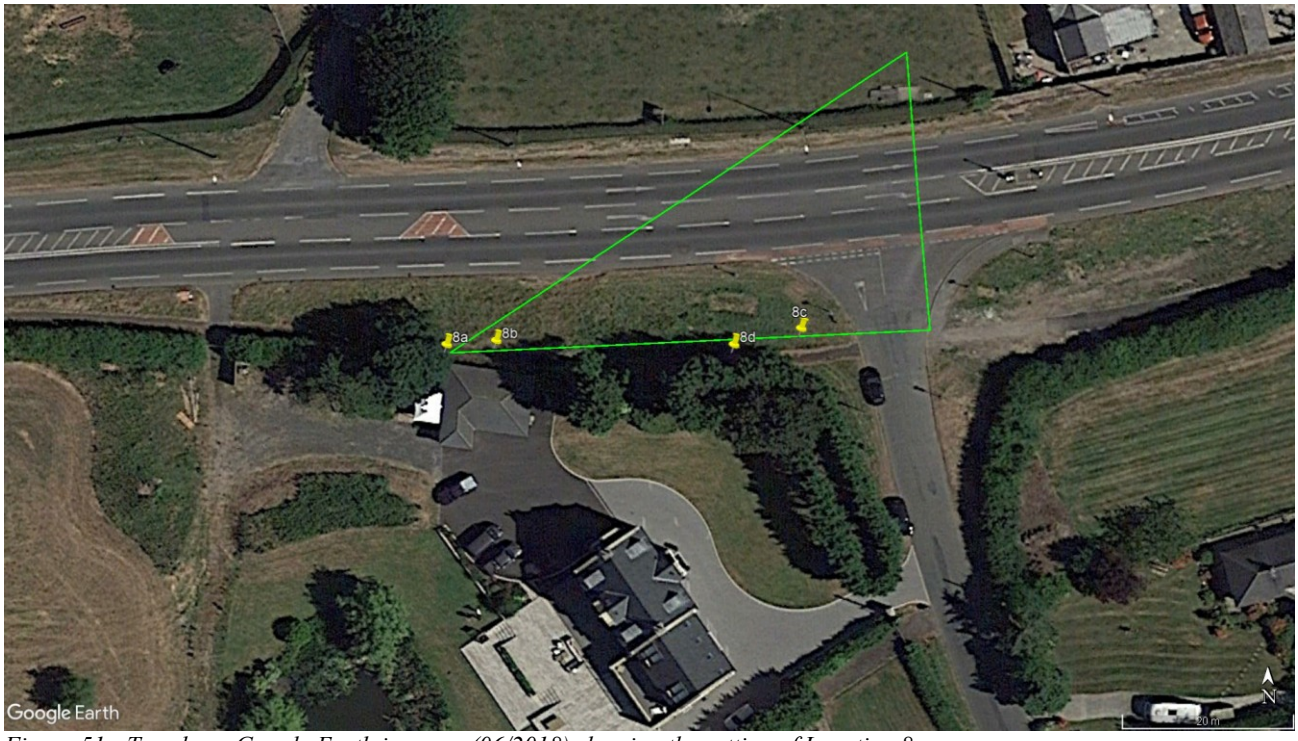

Figure 51 - Top-down Google Earth imagery (06/2018) showing the setting of Location 8.

Located along the southern embankment of Preston New Road (A583). The green polygon indicates the approximate viewing direction of the ground photograph in Figure 53. Approximate locations for the four images are included for context. The image illustrates the relationship between the carriageway, embankment slope, pedestrian route, and adjacent land. A disturbance pattern is visible within the embankment near the junction with Westby Road.

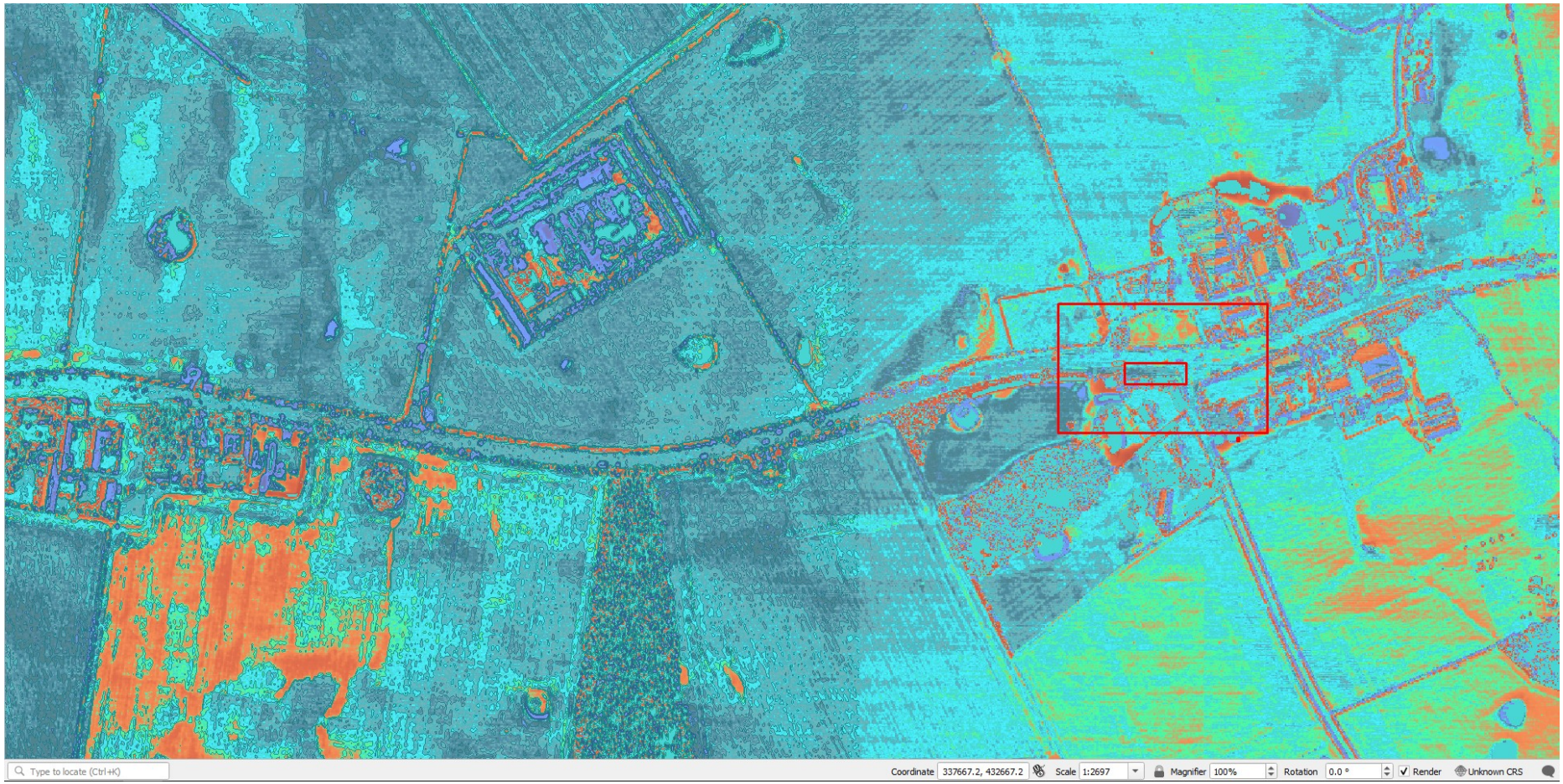

Figure 52 - Location 8: LiDAR elevation change context (2018-2022)

LiDAR elevation differencing highlights a zone of relative surface change along the southern embankment of the A583 at Location 8. Localised elevation variation is present within the embankment face and adjacent verge, consistent with subtle ground adjustment rather than uniform settlement. The geometry of the change is not aligned with road construction joints or verge maintenance boundaries.

Figure 53 - Ground photograph of embankment and pedestrian route at Location 8a (05/01/2026)

Ground photograph taken facing east, showing the pedestrian path and adjacent grassed embankment at Location 8. A narrow linear depression is visible within the grassed slope, extending downslope toward the path. The feature is not associated with a service trench, path construction joint, or visible drainage asset and appears to reflect localised ground movement within the embankment material. (Approx. location: 53.78620 N, -2.944159 W facing East)

Figure 54 - Removed in v1.1
This figure has been removed from the evidential sequence. The feature previously shown here has been reclassified as likely urban debris or exposed hard material rather than a ground-formation feature. It is therefore no longer relied upon in this report.

The following image shows the same location from the opposite direction.

Figure 54 - Opposite-direction view of embankment deformation at Location 8c.

Ground photograph facing west along the A583, showing the same section of embankment. From this perspective, deformation upslope from the path is more clearly expressed. A pale patch is visible on the footpath within the centre of the depression identified in Figure 52. (Approx. Location 53.786215 N, -2.943485 W facing West)

Figure 55 - Pale mineral residue within the depression at Location 8d.

Pale mineral residue within the depression is consistent with repeated low-rate seepage, where dissolved material is deposited at the surface following evaporation. This observation supports interpretation of focused subsurface water movement rather than surface runoff (Approx. Location 53.786192 N, -2.943611 W facing West)

Interpretive note (Location 8)

Although Location 8 is not associated with a mapped surface watercourse, the presence of LiDAR-detected elevation change, linear surface cracking, and active seepage demonstrates that subsurface water movement and ground response extend into engineered embankments. This location provides an important contrast to channel-adjacent sites, showing that similar processes operate along infrastructure margins within the wider hydrological corridor.

4.8.1 - Summary of observations (Location 8)

Location 8 demonstrates that surface deformation and subsurface water emergence and expression are present along an engineered embankment associated with the A583, despite the absence of a mapped surface watercourse. The combination of LiDAR-detected elevation change (2018-2022), linear surface cracking, and active seepage indicates that this location is responding to local ground and hydrological conditions rather than superficial wear, maintenance activity, or surface runoff alone.

The geometry of the deformation and seepage is inconsistent with construction joints, verge works, or service alignments, and instead reflects focused subsurface water movement and localised ground adjustment within the embankment material. This reinforces observations made elsewhere in the study area that ground response is not confined to open drainage channels, but also affects engineered slopes and infrastructure margins within the broader corridor.

Location 8 therefore provides additional evidence that the processes influencing ground stability and water movement operate across both natural and engineered environments, supporting interpretation of distributed, system-wide ground sensitivity rather than isolated site-specific issues.

4.9 Location 9

Location 9 is situated at the junction of Preston New Road and Moss House Lane, immediately adjacent to the southern verge of Preston New Road and west of the Moss House Lane carriageway. The location comprises a grassed verge and informal green space bordered by road infrastructure, signage, and adjacent commercial land use.

This site was selected for investigation due to the presence of persistent surface irregularities, ground depressions, and anomalous surface features occurring within a constrained and trafficked junction environment, where routine maintenance would normally limit the persistence of such features.

Figure 56 - Location 9 context and setting (Google Earth, 05/2020)

Top-down Google Earth imagery showing the junction of Preston New Road and Moss House Lane and the position of Location 9. The image illustrates the spatial relationship between the road junction, grassed verge, signage, and adjacent parking and commercial areas. The location occupies a transitional zone between highway infrastructure and informal green space.

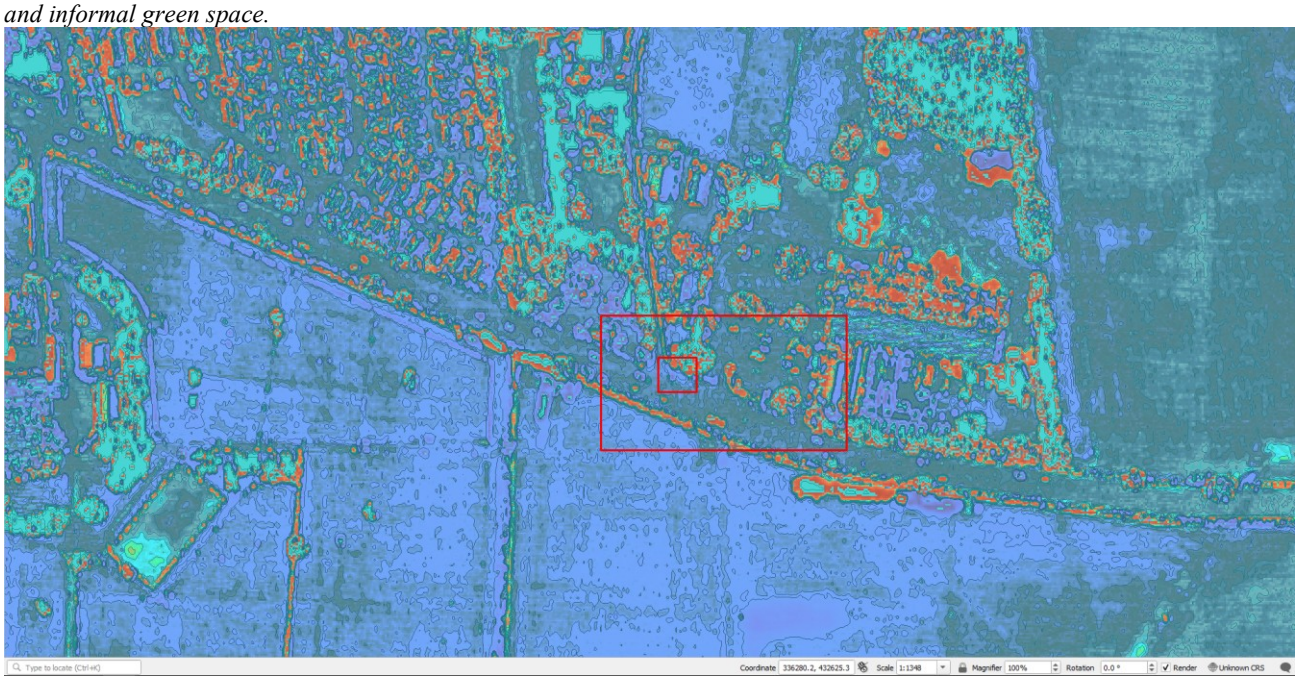
Figure 57 - LiDAR elevation change context at Location 9 (2018-2022)

LiDAR elevation differencing highlighting localised surface variability within the grassed verge and junction margins at Location 9. Zones of relative elevation change are irregularly distributed and not aligned with road construction edges, kerbs, or service corridors, suggesting localised ground response rather than uniform settlement or resurfacing effects.

Ground-based imagery from 2025 and 2026 provides additional detail on surface condition and

temporal change at this location.

Figure 58 - Location 9(a) - Ground photograph of verge surface irregularities at Location 9 (23/05/2025)

Ground photograph taken facing south-southeast adjacent to the junction of Preston New Road and Moss House Lane. Areas of reduced grass cover and shallow surface depressions are visible within the verge. The street sign visible in the image exhibits a noticeable lean, consistent with local ground instability rather than impact damage. The distribution of surface voids corresponds spatially with depressions identified in LiDAR analysis. (Approx. Location 53.786352 N, -2.96901 W facing East-South-East)

Figure 59 - Location 9 (b) Ground photograph showing flat surfaced feature within Location 9.

Ground photograph showing a flat slab at the surface and a subsurface access cover within the grassed verge at Location 9. The feature is partially exposed and surrounded by uneven ground, surface voids, and disturbed turf. While the surface appears artificially planar, their setting within an area of broader surface deformation, mounding, and LiDAR-detected elevation change indicates response to local ground movement rather than a stable or intact infrastructure element. The surrounding surface irregularities suggest ongoing or progressive ground adjustment at this location. (Approx. Location 53.786332 N, -2.968942 W facing North-East)

Figure 60 - Location 9(c) Ground photograph showing surface mounding and redistribution at Location 9 (08/01/2026)

Photograph taken from the same general area looking northeast along Preston New Road. Low, irregular mounds of disturbed soil are distributed across the verge in locations previously occupied by surface voids and depressions. The pattern suggests ongoing ground adjustment or material migration rather than isolated animal activity or landscaping works. (Approx. location 53.786261 N, -2.968828 W facing West)

4.9.1 Summary of observations (Location 9)

Location 9 documents surface deformation and ground disturbance occurring within a landscaped roadside and junction setting at the intersection of Preston New Road and Moss House Lane. Observed features include recurring surface voids, low mounding, uneven ground texture, and deformation affecting fixed infrastructure such as signage, all of which persist across multiple observation periods.
The correspondence between ground-level observations and LiDAR-detected elevation change indicates that the surface expressions at this location are not isolated or transient features. Their distribution across maintained public space, and their recurrence over time, suggest localised ground adjustment rather than routine landscaping effects or isolated surface damage.

Location 9 provides an important intermediate context between engineered embankment settings and active drainage-channel responses documented elsewhere in the study area. The observations demonstrate that surface expressions associated with subsurface processes can manifest within managed and publicly accessible environments, where such features might otherwise be assumed to be superficial or maintenance-related.

Taken together, the features documented at Location 9 reinforce the interpretation that ground response within the wider study area is distributed, spatially coherent, and not confined to agricultural land or formal watercourse margins. This location therefore supports the broader pattern of system-wide ground sensitivity identified across the Preston New Road corridor.

4.10 Location 10

Location 10 is situated approximately 80 m north of Peel Hill Bridge*, which carries Preston New Road over the Main Drain, and approximately 150 m north-east of Location 9. The location lies within a residential and landscaped setting immediately adjacent to the Main Drain corridor, north of the A583.

** (Bridge inscription notes "Rebuilt 1905"; included here for location reference only.)*

This location was selected due to the presence of surface disturbance and anomalous ground features identified in aerial imagery and LiDAR elevation differencing, occurring in close proximity to residential properties and maintained open space. Its position relative to both the Main Drain and previously documented locations provides an important downstream and cross-corridor comparison within the study area.

Figure 61 - Top-down Google Earth imagery showing Location 10 in relation to Location 9, Preston New Road, and the Main Drain corridor (06/2022).

The exact UAV position at the time of image capture is indicated for reference (DJI_0554), providing spatial accuracy for subsequent aerial and ground imagery presented in this section

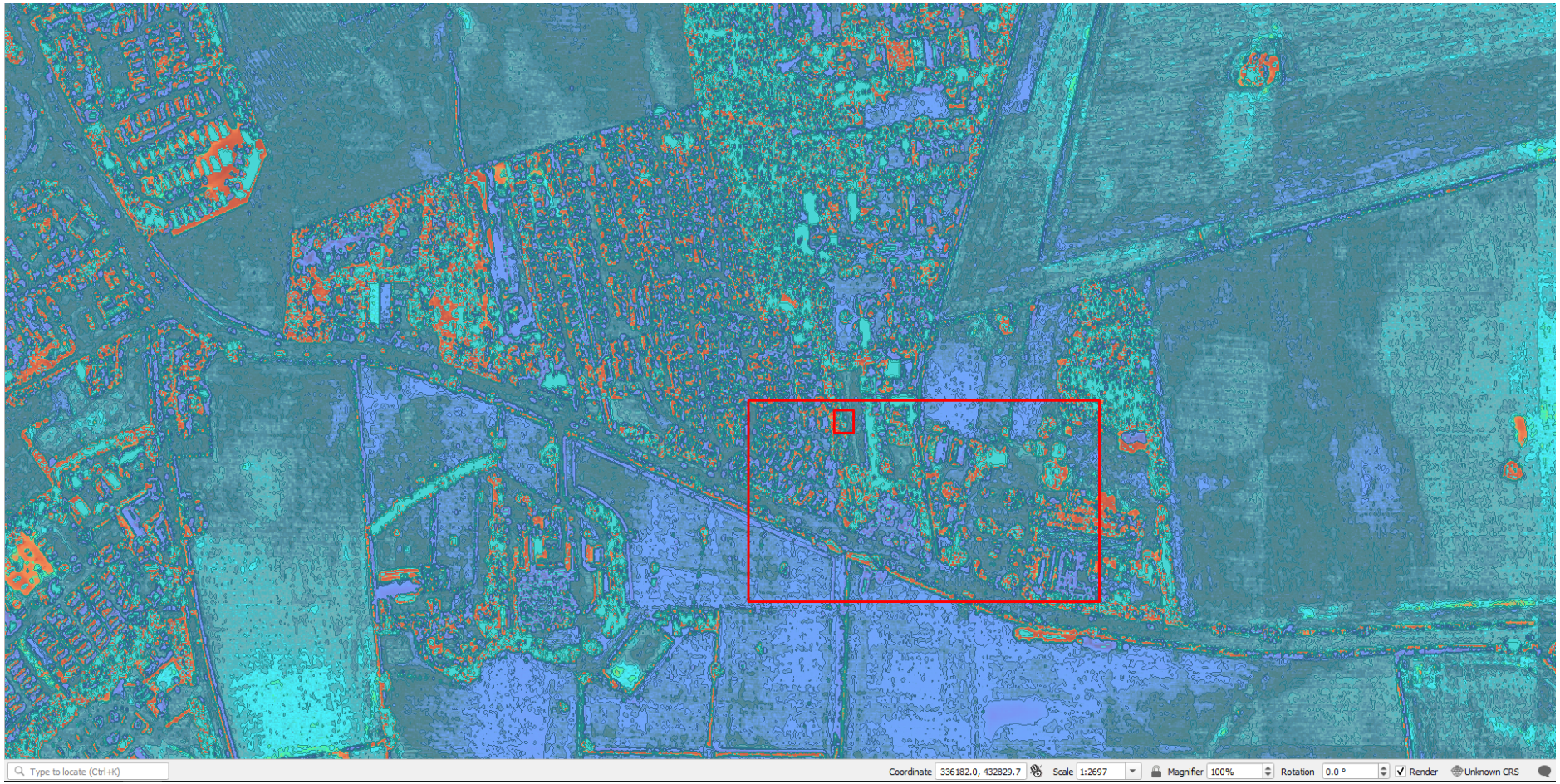

Figure 62 - LiDAR elevation change context at Location 10 (2018-2022).

LiDAR elevation differencing highlighting localised areas of relative surface change within and adjacent to Location 10. The pattern of elevation change is spatially coherent with features observed in aerial and ground imagery and is not aligned with formal landscaping boundaries or known drainage assets.

Figure 63 - Bank-face discharge at Location 10 (04/01/2026).

Ground photograph showing a discrete bank-face discharge point along the Main Drain, with visible orange-brown sediment emerging at the waterline.

Figure 64 - Elevated water level partially occluding lower discharge points (12/01/2026).

Higher water levels within the Main Drain obscure the lower portion of the bank face; however, openings within the bank structure remains visible above the waterline.

Figure 65 - Receding water level with renewed sediment expression (16/01/2026).

Lower water levels reveal the bank-face openings again, with orange sediment still present at and below the discharge points.

Figure 66 - Elevated water level within the Main Drain (19/01/2026).

Ground photograph showing increased water levels partially inundating the bank face at Location 10, coincident with continued sediment expression higher on the bank.

Figure 67 - Progressive change in bank-face configuration at Location 10 (02/02/2026).

The left-hand opening visible in previous figures has closed, while sediment emergence is now observed higher on the bank. Additional new openings and fresh staining are visible to the left, indicating ongoing adjustment and reorganisation of subsurface discharge pathways.

Figure 68 - Ground photograph of Main Drain bank and staining (04/02/2026)

A newly observed seepage expression is present south of the initial cluster of staining along the bank. Red box shows the location of the zoomed image in the following Figure.

Figure 69 - Intermediate view of seepage feature shown in Figure 68.

Intermediate-range image showing surface wetness and flow alignment across the bank face, providing context for the close-range detail shown in Figure 71

Figure 70 - Close-range detail of seepage feature shown in Figure 69.

Close-range image illustrating fine-scale flow patterning and multiple small emergence points within the bank face. This view is provided to distinguish active seepage expression from superficial debris or vegetation.

A detailed index of image dates and observed qualitative water levels associated with Figures 64–71 is provided in Appendix B.

Figure 71 - Aerial imagery showing surface conditions at Location 10.

This image provides spatial context for the ground-level observations presented in Figures 64-71 and illustrates the relationship between bank disturbance and adjacent maintained land. (Approx. Location 53.787419 N, -2.970334 W facing East)

4.10.1 - Summary of observations (Location 10)

Location 10 documents a sequence of bank-face discharge features along the Main Drain that exhibit clear temporal evolution over a period of weeks. The repeated opening, partial occlusion, re-emergence, and migration of sediment-bearing discharge points demonstrate active and dynamic subsurface water movement rather than a static or isolated surface staining phenomenon.

The observed behaviour is closely linked to fluctuating water levels within the Main Drain and is spatially consistent with areas of LiDAR-detected elevation change identified between 2018 and 2022. The discharge features are not attributable to routine landscaping, bank maintenance, or isolated material exposure, and instead indicate progressive reorganisation of subsurface flow pathways within the bank.
Given its proximity to residential properties, maintained open space, and previously documented locations upstream and across the corridor, Location 10 represents a critical example of active ground and hydrological response within the study area.

The observations here reinforce the interpretation that ground disturbance and subsurface water movement are ongoing, spatially connected processes rather than isolated or benign surface expressions.

4.10.2 - Summary of Locations 8 - 10: Infrastructure-Adjacent and Channel-Connected Ground Response

Locations 8-10 document a progression of ground disturbance and subsurface water expression across engineered, landscaped, and open-channel environments within the same drainage corridor as Preston New Road (A583). Although differing in immediate setting and surface use, the locations share common characteristics in geometry, behaviour, and temporal evolution.

Location 8

Demonstrates that ground deformation and subsurface water movement are present within an engineered roadside embankment and pedestrian verge, despite the absence of a mapped surface watercourse. LiDAR elevation differencing (2018-2022) identifies localised surface change within the embankment, coincident with linear surface cracking and active seepage observed on the ground. The deformation geometry is not aligned with construction joints, verge maintenance limits, or service corridors, indicating localised ground response and focused subsurface flow within the embankment material.

Location 9

Situated at the junction of Preston New Road and Moss House Lane, extends these observations into a publicly accessible landscaped and roadside setting. Ground observations across multiple dates document recurring surface disturbance, including voids in grass cover, low mounding, and deformation affecting fixed features such as signage. These features correspond spatially with LiDAR-detected elevation change and are not attributable to routine maintenance, landscaping, or isolated infrastructure works. The location provides an intermediate link between engineered roadside environments and downstream drainage features.

Location 10

Represents the most direct expression of subsurface water emergence within the study sequence. Situated immediately adjacent to the Main Drain, this location exhibits repeated and evolving bank-face discharge points producing orange-brown sediment. A time-series of ground photographs collected between early January and early February 2026 documents changes in discharge position, number of openings, sediment volume, and staining extent in response to fluctuating water levels. Some discharge points close while new ones emerge higher on the bank, indicating ongoing reorganisation of preferential flow pathways rather than a static or isolated condition. LiDAR elevation differencing identifies localised surface change within the same area, spatially coherent with the observed bank-face activity.

Taken together, Locations 8-10 demonstrate that ground response and subsurface water movement within the study area are not confined to natural watercourses alone, but affect engineered embankments, landscaped public spaces, and open drainage channels within the same corridor. The observations show repeatability, spatial coherence, and temporal evolution across multiple land uses and infrastructure types, supporting interpretation of distributed and active ground sensitivity rather than isolated, site-specific anomalies.

4.11 Location 11

Location 11 is situated approximately 650 m west of the Preston New Road well pad and lies within the same low-relief, drainage-dependent agricultural setting described in Section 3. This location is included because it exhibits multiple, spatially related surface features involving ponding, redistribution of ponded water beyond the original pond margin, seepage-associated surface saturation and deformation, and a closed surface depression, all occurring within a single, confined field unit.

The observations at this location are notable because they combine surface water redistribution, bank instability, and field-scale surface deformation within a single setting. While the broader report focuses on watercourse interaction and bank behaviour, the features documented here provide additional context for understanding how surface water and near-surface ground conditions interact across the wider drainage landscape.

This location is presented for descriptive and contextual purposes only. No inference is made regarding subsurface pathways, driving mechanisms, or causation.

Figure 72 - Google Earth context and oblique imagery orientation (06/2024)

Google Earth imagery showing the location of Location 11 relative to surrounding fields and infrastructure. Polygons indicate the approximate viewing direction of the oblique aerial images presented in Figures 75-78 across the field surface, while Figure 74 looks south toward the bank of this field at Carr Bridge Brook. This figure provides spatial orientation and context for the features described below.

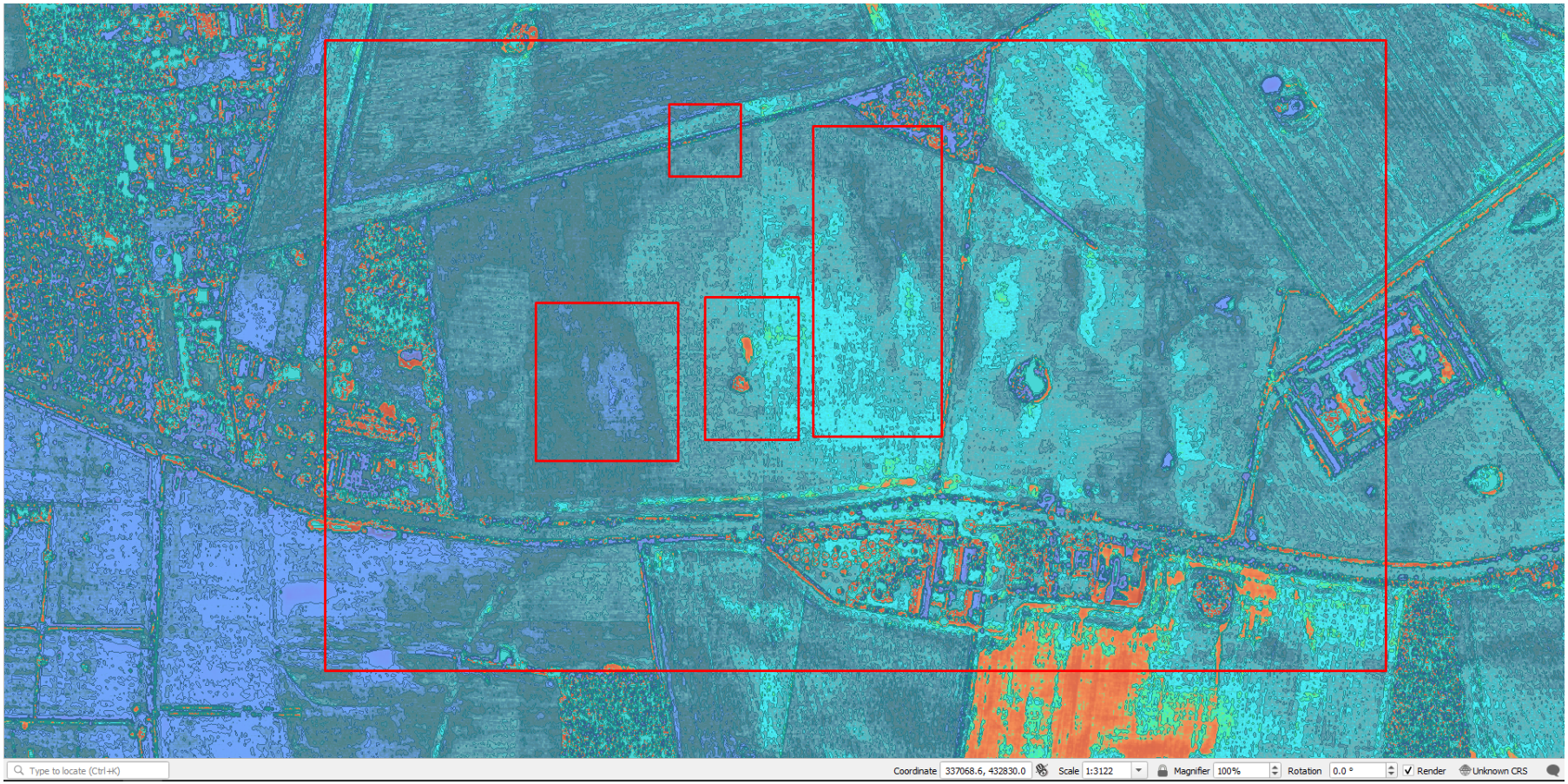

Figure 73 - LiDAR elevation differencing (2018-2022) for Location 11, with four sub-areas of interest delineated.

- *The left-hand box highlights a closed surface depression visible in both LiDAR and aerial imagery, aligned broadly north-south.*
- *The central box corresponds to the hexagonal pond and an area affected by water-surface reflection artefacts, and is included to distinguish data limitations from genuine surface change.*
- *The right-hand box captures an elongate zone of relative elevation change.*
- *The northernmost box represents an area of bank collapse along Carr Bridge Brook.*

Inspection of the LiDAR elevation differencing using measurement tools indicates that the closed depression identified in the left-hand box corresponds to a relative elevation change on the order of ~0.15 m. This value is provided for scale only and is not used to infer depth, volume, or mechanism.

Figure 74 - Location 11a - Pond overtopping and northward water expansion

Aerial image showing a hexagonal pond within Location 11 that shows loss of pond containment and has breached its northern margin. Ponded water is visible extending onto the adjacent ground surface to the north, indicating redistribution of surface water beyond the original pond boundary. (Approx. Location 53.786659 N, -2.960622 W facing North-North-East)

Figure 75 - Location 11b - Ground surface expression aligned with LiDAR depression

Low-altitude aerial image showing surface conditions corresponding to the elongate depression identified in Figure 74. The ground surface exhibits a broad, shallow depression trending approximately North-South.(Approx. Location 53.786584 N, -2.960522 W facing West)

Figure 76 - Location 11c - Seepage associated surface saturation and deformation northwest of the pond.

Image showing a further shallow surface depression located approximately 150-200 m northwest of the pond shown in Figure 75. The area exhibits signs consistent with spring seepage or groundwater emergence, expressed as surface saturation and subtle surface lowering. (Approx. Location 53.789593 N, -2.960512 W facing South-South-East)

Figure 77 - Location 11d - Bank collapse along Carr Bridge Brook, north of Location 11.

Aerial image showing localised bank failure and material loss located along Carr Bridge Brook at the north-eastern edge of the field-scale depression identified in Figure 74 & 76, as shown by LiDAR elevation differencing. The feature illustrates bank instability within the same local drainage corridor and provides context for the interaction between surface depressions and adjacent watercourse behaviour. (Approx. Location 53.789593 N, -2.962116 W facing South-South-East)

The spatial alignment of this bank failure with the field-scale depression suggests that surface and near-surface processes expressed within the field extend to, and interact with, the adjacent watercourse. Additional aerial imagery from this reach shows localised sediment mounding and redistribution along the same bank section, consistent with ongoing bank adjustment rather than a single failure event.

4.11.1 - Summary of observations (Location 11)

Location 11 documents a cluster of surface features that together indicate active redistribution of surface water and associated ground response within a single field unit. These include loss of pond containment and redistribution of surface water beyond the original pond margin, shallow but spatially coherent surface depressions, and areas exhibiting surface conditions consistent with seepage-associated saturation and deformation.

The redistribution of ponded water coincides with visually apparent surface wetness and subtle ground deformation observed in aerial imagery. The spatial relationship between these features

suggests interaction between surface water and near-surface ground conditions, without inferring a specific subsurface pathway, material property change, or driving mechanism.

The coincidence of these features with zones of relative elevation change identified through LiDAR analysis suggests that surface water behaviour and ground condition are interacting dynamically at this location. While no causation is inferred, the observations demonstrate that changes in water distribution are occurring beyond defined channel boundaries and are expressed across the field surface.

For the purposes of this report, Location 11 is included to illustrate how surface water and ground response can manifest away from formal watercourses while remaining relevant to considerations of drainage performance, bank stability, and surface-subsurface interaction within a low-relief, drainage-dependent setting. More detailed analysis of ground deformation mechanisms at this location is beyond the scope of the present submission and may be addressed separately. The observations are presented as a spatially and temporally coherent pattern rather than as isolated defects.

4.12 Location 12

Location 12 provides spatial continuity between previously documented observations at Locations 3, 9, and 11. The area lies within the intervening low-relief agricultural ground south of the A583, where aerial imagery and LiDAR elevation differencing indicate surface wetness, subtle ground disturbance, and drainage-related expression consistent with the wider patterns described in this report. The location was selected following review of aerial imagery and LiDAR elevation differencing, which together indicate surface wetness, subtle ground deformation, and downslope water movement occurring outside formally mapped watercourses.

Observations at this location are presented to illustrate how ground response and subsurface water expression manifest across intervening fields, reinforcing the interpretation that observed processes are spatially connected and operate across the wider landscape rather than being confined to discrete sites. This location does not introduce new mechanisms or interpretations, but serves to integrate and contextualise previously described observations within a continuous corridor setting.

Figure 78 - Google Earth overview of Location 12 (10/2024).

Overview of the intermediate fields between Locations 3, 9, and 11, showing low-lying agricultural land with subtle tonal variation and vegetation stress consistent with repeated surface wetness. Pins labelled with ".JPG" indicate representative UAV image capture locations referenced in this section.

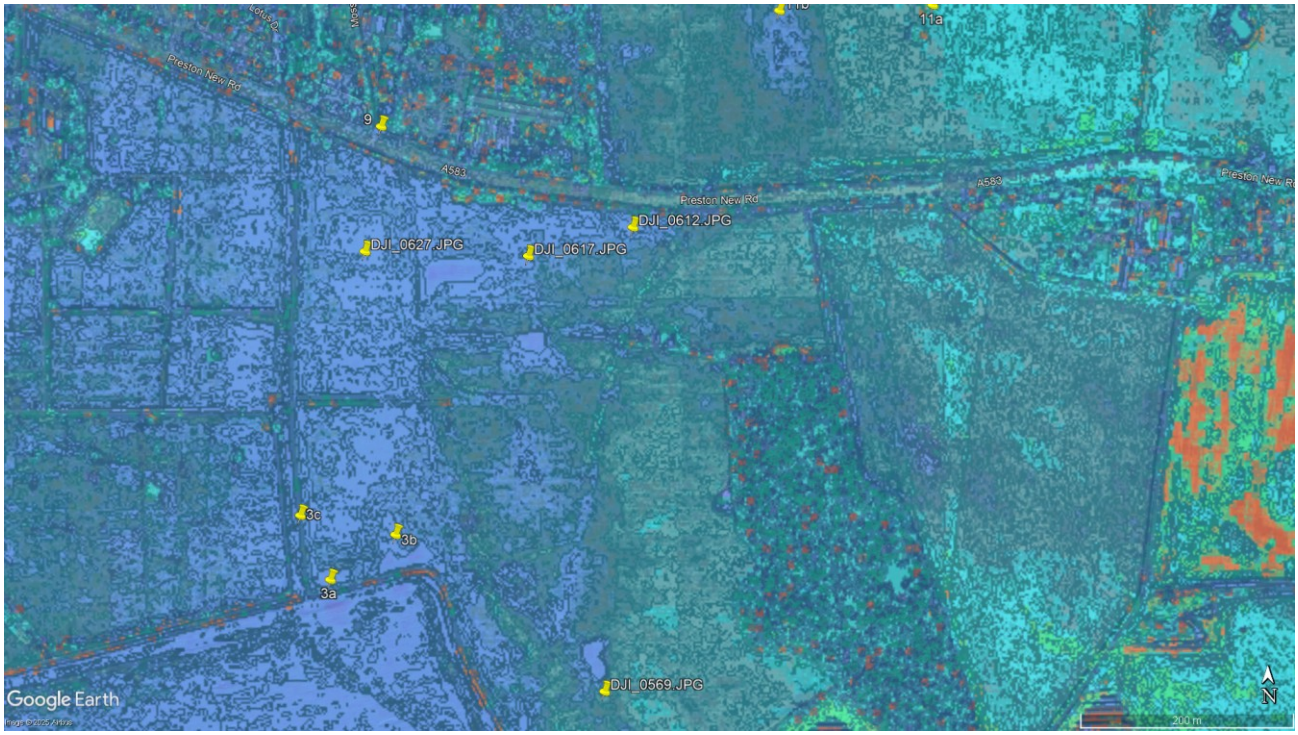

Figure 79 - Location 12: Google Earth view overlaid with LiDAR elevation differencing (2018–2022).

LiDAR differencing highlights broad zones of elevation change coincident with low-relief areas and subtle linear features visible in aerial imagery. These patterns correspond spatially with surface wetness and disturbance described in the following figures.

Figure 80 - Location 12a: Aerial image looking east across fields south of the A583.

Image shows linear surface wetness and discoloured water expression consistent with downslope seepage emerging within the field interior. Surface water patterns align with subtle ground depressions extending away from the road corridor. The pond documented previously at Location 11 is visible in the mid-distance, with apparent alignment coinciding with surface water expression on the south side of the A583. (Approx. Location 53.785248 N, -2.969237 W facing East)

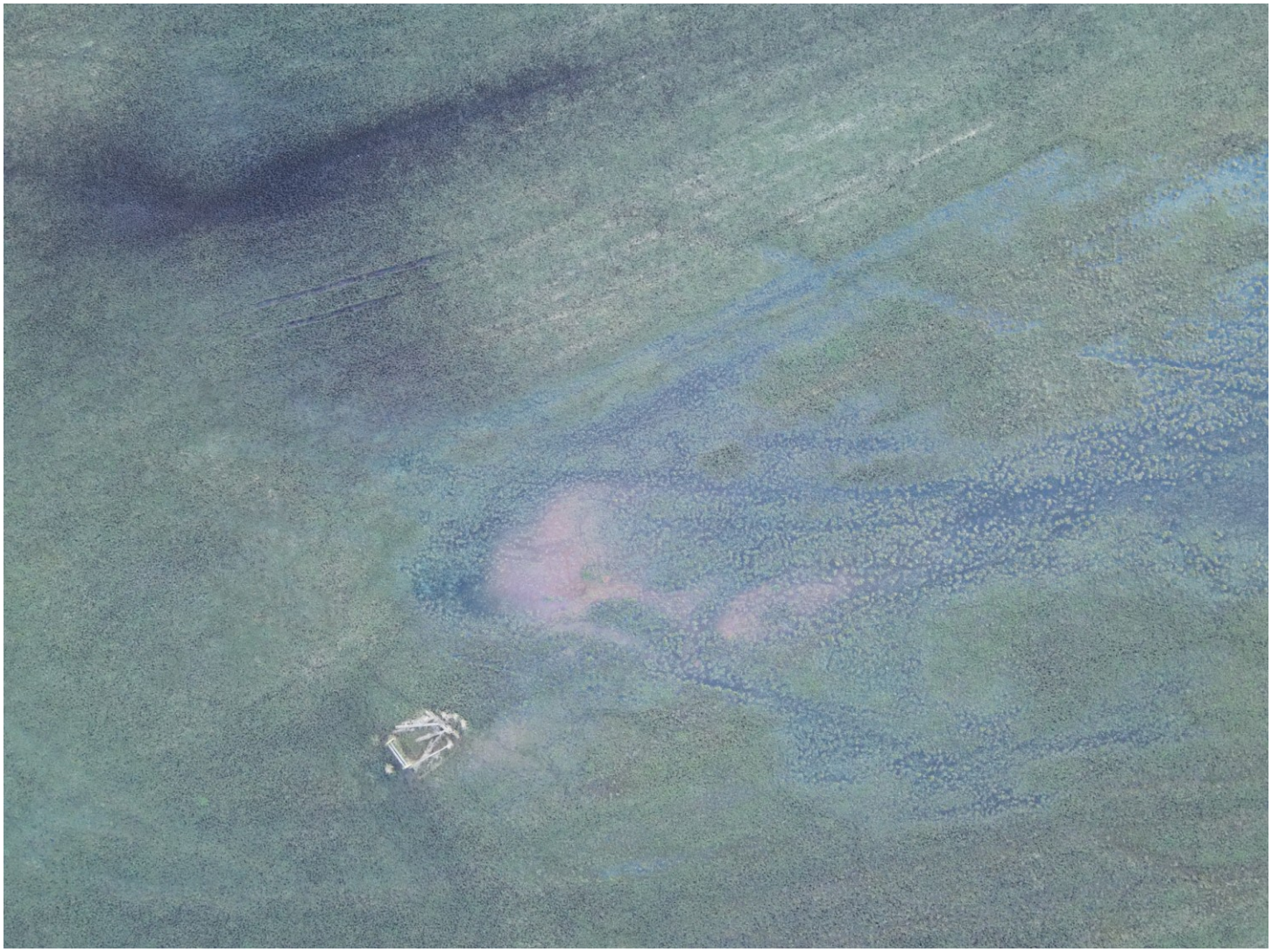

Figure 81 - Location 12b: Surface ponding and sediment staining within low-relief field.

Localised surface ponding is accompanied by sediment staining and saturated soil conditions. The geometry and distribution of wet areas are consistent with elevation change identified in LiDAR differencing and indicate persistent surface expression rather than short-lived rainfall runoff. (Approx. Location 53.785209 N, -2.966898 W facing South-West)

Figure 82 - Location 12c: Surface disturbance and shallow water accumulation adjacent to the A583.

This image shows shallow surface water accumulation associated with subtle ground disturbance extending away from the road margin into the field. Areas of past road patching are present adjacent to the field disturbance. Similar surface patterns are observed elsewhere in the study area, suggesting a recurring spatial association between ground deformation and surface water emergence rather than isolated or site-specific features. (Approx. Location 53.785209 N, -2.966898 W facing North-East)

Figure 83 - Location 12d: Fluid-filled depression and associated vegetation stress.

A shallow, fluid-filled depression is visible within the field interior, accompanied by vegetation stress and surrounding discolouration. The form and setting of the feature are consistent with other surface expressions documented within the corridor, indicating ongoing interaction between subsurface water movement and near-surface ground response.

4.12.1 Summary of observations (Location 12)

Location 12 documents surface wetness, shallow ponding, sediment staining, and subtle ground deformation occurring within low-relief agricultural fields situated between previously described locations. Aerial imagery and LiDAR elevation differencing demonstrate that these features are spatially coherent with downslope water movement and broader zones of elevation change, despite the absence of formally mapped surface watercourses.

The observations reinforce the interpretation that ground response and subsurface water expression operate across intervening fields within the study corridor, linking infrastructure-adjacent settings with downstream channel-connected expressions. Location 12 therefore provides integrative context, supporting the view that observed processes are distributed across the landscape rather than confined to isolated sites.

Having established the observable characteristics and persistence of these surface expressions, it is appropriate to consider what these observations imply for systems of monitoring, oversight, and escalation.

5. Discussion and Implications

The preceding sections document observable surface and near-surface features, their spatial distribution, and their evolution over time, without attributing cause or responsibility.

The following section does not seek to assign fault, determine regulatory compliance, or evaluate the performance of any specific organisation. Instead, it considers how the observed characteristics of these surface expressions — including their persistence, spatial coherence, and occurrence beyond formal asset boundaries — interact with existing approaches to monitoring, inspection, and escalation.

This discussion is included to provide contextual relevance to the observations presented, and to support informed consideration of whether current frameworks are equipped to recognise and respond to the types of ground behaviour documented herein.

The observations documented in this report are relevant to statutory environmental oversight irrespective of the ultimate subsurface cause. Matters of bank stability, groundwater and surface-water interaction, seepage into watercourses, sediment mobilisation, iron-rich or discoloured discharge, and the adequacy of monitoring to reliably detect and classify such phenomena fall squarely within responsibilities relating to protection of the water environment and flood risk management.

The focus of this section is therefore not attribution of cause, but consideration of whether existing monitoring, classification, and oversight frameworks are sufficient to recognise, interpret, and respond to the types of surface and near-surface behaviour documented.

The observations documented at Locations 8-10 represent a qualitative shift in surface expression, rather than in underlying process, from earlier sections of this report. Whereas preceding locations primarily describe surface response within agricultural and drainage-channel settings, these later locations build on patterns first identified at Locations 1-7, extending them from agricultural and channel-margin settings into engineered infrastructure, landscaped public space, and actively managed drainage corridors.

Across these locations, the evidence shows that ground response is not static. Instead, it evolves over time, with surface expressions appearing, changing position, intensifying, and in some cases closing or migrating. This behaviour is observed across multiple surface types and land uses and is spatially coherent with zones of elevation change identified through LiDAR analysis. Importantly, several of these features were documented repeatedly over weeks and months, rather than representing transient or single-event phenomena.

Seasonal rainfall and antecedent wet conditions may influence the timing and surface expression of some features described. However, the persistence, spatial coherence, and recurrence of observed seepage, surface disturbance, and elevation change across multiple years, land uses, and hydrological conditions indicate that rainfall alone is unlikely to be a sufficient explanatory mechanism. Rainfall is therefore treated as a potential modulating factor rather than a primary driver in the interpretations presented.

These observations raise questions not of causation, but of detectability and classification. In particular, the evolving bank-face discharge documented at Location 10 illustrates a class of surface expression that may not trigger conventional monitoring thresholds or compliance responses, yet nonetheless reflects active subsurface processes interacting with surface drainage systems. Where such features are classified narrowly or dismissed as benign surface phenomena,

there is a risk that meaningful early indicators of ground or hydrological instability are overlooked.

The locations presented here also highlight a limitation of monitoring frameworks that focus on discrete assets or predefined pathways. Ground response observed within embankments, verges, junctions, and channel margins demonstrates that subsurface processes can manifest beyond expected receptors and outside the footprint of formal monitoring infrastructure. In such contexts, reliance on static models or confirmatory monitoring may fail to capture the distributed and progressive nature of ground adjustment.

This section therefore considers the implications of the observations presented for monitoring design, regulatory response, and the assessment of ongoing ground and watercourse stability within the study area. The emphasis is not on attributing cause, but on evaluating whether existing frameworks are sufficient to detect, interpret, and respond to the types of surface and subsurface behaviour documented in this report.

5.1 Implications for Monitoring Design and Sensitivity

The observations documented in this report indicate that ground response and subsurface water movement within the study area can manifest in forms and locations that fall outside the scope of conventional monitoring frameworks. In particular, the features observed at Locations 8-10 demonstrate that significant surface expressions may develop within engineered embankments, landscaped verges, and channel margins without triggering predefined thresholds or alarms.

Several characteristics of the observed features reduce their likelihood of detection under standard monitoring regimes. These include low-magnitude but spatially coherent surface deformation, gradual or episodic evolution over weeks rather than abrupt onset, and expression at the interface between surface and subsurface systems rather than as discrete exceedances within monitored assets. Where monitoring is designed primarily to confirm expected behaviour or to detect acute failure, such signals may be recorded but not recognised as significant.

The time-series observations at Location 10 are particularly instructive in this regard. Repeated bank-face discharge, migration of emergence points, and changing sediment expression occurred over a period of weeks, with features opening, closing, and reappearing in response to fluctuating water levels. Such behaviour may not be captured by snapshot inspections or periodic reporting, especially where observations are framed around the presence or absence of contamination rather than the dynamics of flow and ground response.

Additionally, the spatial distribution of features across Locations 8-10 illustrates that subsurface processes are not confined to predefined receptors such as monitoring boreholes, culverts, or surface water sampling points. Ground response expressed within verges, junctions, and embankments may therefore fall between monitoring locations, creating structural blind spots even where formal monitoring networks are in place.

These observations suggest that monitoring sensitivity is influenced not only by instrument placement and sampling frequency, but also by the conceptual model used to interpret signals. Where monitoring frameworks assume static conditions or narrowly defined pathways, evolving and distributed surface expressions may be misclassified as benign or incidental. As a result, early indicators of ground or hydrological instability may be present but remain operationally invisible.

The findings presented here indicate a need to consider whether existing monitoring approaches are sufficiently exploratory to detect unanticipated surface-subsurface interactions, particularly in

low-lying, drainage-dependent landscapes where small changes in ground condition can produce disproportionate surface effects.

5.2 Signal Classification and the Risk of False Negatives

The effectiveness of any monitoring framework depends not only on the detection of signals, but on how those signals are classified, interpreted, and acted upon. The observations documented at Locations 8-10 indicate that surface expressions associated with subsurface water movement and ground response may be observed yet discounted through categorisation processes that frame them as benign, isolated, or unrelated to wider system behaviour.

Several of the features described in this report exhibit characteristics that make them vulnerable to misclassification. These include the absence of obvious acute impacts, low apparent contaminant concentrations, and visual similarity to naturally occurring phenomena such as iron-rich seepage or minor surface wetness. Where assessment criteria focus primarily on chemical exceedance, acute failure, or immediate environmental harm, dynamic physical processes may be acknowledged but not treated as decision-relevant.

The time-series evidence at Location 10 highlights this risk. Bank-face discharge points producing orange-brown sediment were observed repeatedly over several weeks, with emergence points opening, closing, and migrating in response to changing water levels. While such features may be readily labelled as iron ochre staining in isolation, the observed temporal evolution, spatial reorganisation, and association with localised ground change indicate an active process rather than a static surface condition. Classification based solely on visual appearance at a single point in time risks obscuring this behaviour.

A further risk arises where responsibility for interpretation is fragmented across regulatory remits or asset boundaries. Features observed within road verges, landscaped areas, or non-designated land parcels may be treated as outside the primary scope of watercourse or groundwater monitoring, even where they are hydraulically connected to monitored systems. In such cases, observations may be logged but not escalated, contributing to a cumulative false negative at the system level.

The distinction between absence of evidence and evidence of absence is particularly relevant in this context. The lack of detected contamination or threshold exceedance does not preclude the presence of ongoing ground adjustment or subsurface flow reorganisation. Where monitoring conclusions are framed narrowly around compliance status, evolving physical processes may remain unaddressed until they manifest as more overt failure or impact.

The observations presented here suggest that signal classification plays a critical role in determining whether monitoring outcomes reflect true system behaviour or a filtered subset aligned with predefined expectations. Without mechanisms to reassess classifications in light of repeated, spatially coherent, or evolving observations, monitoring frameworks risk systematically underestimating ground and hydrological sensitivity in complex, low-gradient environments.

5.3 Implications for Site-Level Oversight and Ongoing Stability

The observations documented across Locations 8-10 have direct implications for how site-level oversight is conducted in low-lying, drainage-dependent environments. In particular, they demonstrate that surface expressions of subsurface processes may occur beyond the boundaries of formal assets and outside areas typically prioritised for inspection, yet still influence the stability and function of the wider drainage system.

At the site level, several features identified in this report would not ordinarily trigger enhanced investigation under routine inspection regimes. These include low-magnitude surface deformation, episodic seepage, and sediment expression that does not immediately affect water quality or flow capacity. However, the repeated occurrence, spatial coherence, and temporal evolution of these features indicate that they represent active processes rather than static or incidental conditions.

The bank-face discharge observed at Location 10 is illustrative of this challenge. The evolution of discharge points over time, including opening, partial occlusion, migration, and re-emergence, reflects ongoing reorganisation of subsurface flow pathways. Such behaviour suggests that ground and bank materials are responding dynamically to hydraulic conditions within the Main Drain, with implications for longer-term bank integrity even in the absence of acute failure.

Site-level oversight that relies on periodic visual inspection or compliance-based checks may therefore underestimate the significance of these processes. Without mechanisms to track change over time or to integrate observations across adjacent land parcels and infrastructure types, early indicators of instability may be logged but not contextualised. This can result in a reactive posture, where intervention occurs only once erosion, collapse, or service disruption becomes apparent.

The proximity of several documented features to residential areas, transport corridors, and maintained public space further underscores the importance of anticipatory oversight. While none of the observations presented here are claimed to constitute immediate hazard, their presence indicates sensitivity within the ground-water-structure system that warrants continued attention. Failure to recognise such sensitivity at the site level increases the likelihood that future responses will be driven by consequence rather than prevention.

Taken together, the findings suggest that effective site-level oversight in this setting requires an approach that recognises evolving ground behaviour, integrates observations beyond formal asset boundaries, and treats repeat or migrating surface expressions as decision-relevant indicators rather than background conditions.

5.4 Governance, Escalation, and Responsibility

The observations presented in this report raise questions not only about monitoring sensitivity and site-level oversight, but also about how responsibility for recognising and acting upon emerging signals is distributed across governance structures. In complex, low-gradient environments where subsurface processes can manifest diffusely and incrementally, the effectiveness of oversight depends on clear pathways for escalation when observations fall outside predefined categories.

Several of the features documented across Locations 8-10 occur in settings that are commonly treated as peripheral to existing regulatory remits. Surface deformation within road verges, landscaped areas, or non-designated land parcels may not fall squarely within the responsibility of any single authority, particularly where impacts are not immediately linked to regulated discharges, exceedances, or asset failure. In such cases, observations may be acknowledged locally but not escalated, as they do not trigger formal thresholds or enforcement criteria.

This fragmentation of responsibility creates a structural risk of inaction. Where planners, regulators, and operators each rely on others to own interpretation of emerging signals, system-level behaviour may go unrecognised. Features that are individually classified as minor, natural, or non-impacting can collectively represent meaningful indicators of ground and hydrological

sensitivity, yet remain operationally invisible due to the absence of a mechanism to integrate observations across domains.

The dismissal of evolving surface expressions as isolated or benign phenomena illustrates this challenge. Where classification frameworks prioritise compliance status or immediate environmental harm, there may be limited scope to reassess earlier conclusions in light of repeat observations or changing conditions. Without formal re-opener mechanisms or adaptive review processes, governance systems risk reinforcing initial interpretations even as evidence accumulates.

Effective escalation requires not only the ability to detect signals, but also the authority to question underlying assumptions when those signals recur or evolve. This includes recognising when observed conditions fall between regulatory categories, and ensuring that such cases prompt interdisciplinary review rather than default dismissal. In the absence of such pathways, responsibility for recognising emergent risk can become diffuse, with no single body accountable for system-level interpretation.

The findings presented here suggest that governance arrangements should be assessed not solely on whether individual standards are met, but on whether they are capable of responding to patterns of behaviour that develop incrementally across space and time. Where oversight structures lack this capacity, the risk is not simply missed non-compliance, but delayed recognition of conditions that may become more difficult or costly to address at a later stage.

6. Conclusions

This report has documented a series of surface and near-surface ground responses across a connected low-lying landscape around Preston New Road, using a structured hierarchy of evidence. Primary reliance has been placed on repeat ground observations, time-series aerial imagery, and LiDAR elevation differencing, with each dataset used to corroborate, rather than substitute for, the others.

Across Locations 1-12, a consistent pattern of ground behaviour has been observed. These include bank erosion, seepage, sediment staining, surface cracking, localised subsidence, circular depressions, mounding, and progressive reorganisation of discharge points. While individual features vary in form and setting, they recur within a shared drainage and infrastructure corridor and exhibit spatial coherence, persistence, and temporal evolution. The findings remain robust to seasonal variability, as the analysis focuses on pattern persistence rather than event-specific responses.

The evidence demonstrates that ground response in the study area is not confined to open watercourses alone. Surface expressions are documented within agricultural fields, roadside embankments, landscaped verges, junctions, and channel margins, including locations adjacent to residential properties and transport infrastructure. Several features evolve over time, with surface expressions appearing, migrating, intensifying, or closing in response to changing hydrological conditions. This behaviour is inconsistent with static, incidental, or purely superficial surface phenomena.

Importantly, this report does not seek to attribute cause. No single mechanism is asserted, nor is responsibility assigned. Instead, the findings demonstrate that subsurface water movement and ground adjustment are active and distributed processes within the study area, capable of producing

observable surface expressions that may fall outside conventional monitoring expectations or regulatory classifications.

The observations raise substantive questions regarding monitoring design, signal interpretation, and governance response. In particular, they illustrate how low-magnitude but evolving features may remain operationally invisible where monitoring frameworks prioritise predefined pathways, static conceptual models, or compliance-based thresholds. Where surface expressions are classified narrowly or dismissed in isolation, there is a risk that meaningful indicators of ground and hydrological sensitivity are overlooked.

The cumulative evidence presented here indicates that confidence in ground stability and drainage performance cannot be based solely on the absence of threshold exceedance or acute failure. Instead, it depends on the capacity of monitoring and oversight systems to recognise and respond to patterns that develop incrementally across space and time, and across multiple land uses and infrastructure types.

On that basis, this report concludes that:

- Ground and subsurface water behaviour within the study area is dynamic, spatially coherent, and ongoing.
- The surface expressions documented are not isolated incidents, but components of a wider system response.
- Existing monitoring and classification approaches may be insufficiently sensitive to detect, contextualise, or escalate such behaviour.
- Continued reliance on static assumptions or confirmatory monitoring risks delayed recognition of conditions that may affect long-term ground stability, drainage integrity, and infrastructure resilience.

These conclusions are offered to support informed regulatory consideration. The observations warrant careful review not because they demonstrate harm, but because they demonstrate uncertainty that is active, observable, and evolving.

6.1 Implications for Regulatory Consideration

The observations documented in this report do not, in themselves, demonstrate harm, causation, or regulatory breach. They do, however, demonstrate the presence of spatially coherent, temporally persistent ground and hydrological behaviour occurring across multiple land uses and infrastructure settings within a defined drainage-dependent landscape.

On that basis, this report supports consideration of whether existing monitoring frameworks, conceptual site models, and inspection regimes are adequately configured to detect and interpret low-magnitude but evolving surface expressions that develop incrementally across space and time. In particular, it raises questions regarding the sensitivity of current approaches where assessment prioritises predefined pathways, static classifications, or threshold-based exceedance, potentially increasing the risk of false negatives.

The appropriate regulatory response to such observations is not predetermined by this document. Rather, the evidence presented here supports the case for review, integration, and, where necessary, refinement of monitoring and oversight practices to ensure that observable patterns of ground and surface water behaviour are neither dismissed in isolation nor overlooked through narrow signal classification.

Appendix A - Location Index and Spatial Referencing

A.1 Purpose and Use of This Appendix

This appendix provides a consolidated spatial index for all observation locations and associated figures presented in Sections 4-6 of this report. It is intended to support:

- Cross-referencing between figures, locations, and narrative text
- Independent spatial verification of observations

Transparent documentation of coordinate sources and limitations
Each entry links a location identifier (e.g. 5a, 10b) to its corresponding figure number(s), image metadata, acquisition date, viewing direction, and spatial coordinates.

This appendix does not introduce new interpretation. It functions as a reference and audit aid, allowing the reader to confirm spatial consistency and trace observations back to original imagery.

A.2 Coordinate Reference and Disclaimer

- Latitude and longitude values are provided in WGS84.
- Eastings and Northings are provided in OSGB36 / British National Grid.
- Where Eastings and Northings were not recorded directly in the field or image metadata, they were derived from WGS84 coordinates using standard geodetic transformation.
- AI-assisted coordinate conversion was used for all Easting's and Northing's; these derived values are intended for spatial referencing and cross-comparison, not for legal boundary definition or engineering design.

Where ambiguity arises, original imagery, WGS84 coordinates, and figure context should be treated as the primary evidence.

Location Index and Spatial Referencing

Location	Figure	Latitude	Longitude	Facing	Easting	Northing	Image	Date	Aerial / Ground	Notes
1a	8	53.77734	-2.961047	ENE	336765	431651	509	28/01/2026	A	
2a	12	53.77989	-2.964604	ENE	336534	431938	541	28/01/2026	A	
2b	14	53.77989	-2.964604	NW	336534	431938	681	28/01/2026	A	
3a	18	53.7825	-2.969205	N	336235	432233	677	28/01/2026	A	UAV location
3b	20	53.78262	-2.968746	N	336265	432246	681	28/01/2026	A	
3c	22	53.78302	-2.970237	E	336168	432292	666	28/01/2026	A	
4a	26	53.79305	-2.972114	E	336059	433410	379	28/01/2026	A	
4b	28	53.79338	-2.971416	NNW	336106	433446	IMG_2018 1022_124	22/10/2018	G	
4c	29	53.79375	-2.971375	N	336109	433487	386	28/01/2026	A	
4d	31	53.79267	-2.971925	NNE	336071	433367	372	28/01/2026	A	
5a	36	53.79398	-2.966135	ESE	336455	433507	415	28/01/2026	A	
5a	37	53.79392	-2.966213	SSE	336449	433501	414	28/01/2026	A	
5b	39	53.79442	-2.963893	NE	336603	433554	427	28/01/2026	A	
6a	42	53.79656	-2.951206	NE	337442	433781	213	28/01/2026	A	
7a	45	53.79077	-2.956884	SE	337059	433142	139	28/01/2026	A	
4.7.2a	49	53.79417	-2.957151	NE	337047	433520	164	28/01/2026	A	
4.7.2b	50	53.79248	-2.950323	ENE	337494	433326	182	28/01/2026	A	Approx. centre
8a	53	53.7862	-2.944159	E	337891	432623	20260105 _085354	05/01/2026	G	
8b	54	53.78622	-2.944031	N	337899	432625	20260105 _085328	05/01/2026	G	
8c	55	53.78622	-2.943485	W	337935	432624	20260105 _085258	05/01/2026	G	
8d	56	53.78619	-2.943611	W	337927	432621	20260105 _085244	05/01/2026	G	
9a	59	53.78635	-2.96901	ESE	336254	432661	20250523 _145034	23/05/2025	G	
9b	60	53.78633	-2.968942	NE	336258	432659	20250523 _145052	23/05/2025	G	
9c	61	53.78626	-2.968828	W	336265	432651	20260108 _142827	08/01/2026	G	
10b	72	53.78742	-2.970334	E	336168	432781	825	10/01/2026	A	
11a	75	53.78666	-2.960622	NNE	336880	432715	289	28/01/2026	A	
11b	76	53.78658	-2.960522	W	336888	432707	288	28/01/2026	A	

11c	77	53.78959	-2.960512	SSE	336892	433041	275	28/01/2026	A	UAV location
11d	78	53.78937	-2.962116	SSE	336735	433000	333	28/01/2026	A	
12a	81	53.78525	-2.969237	E	336210	432640	627	28/01/2026	A	
12b	82	53.78521	-2.966898	SW	336365	432635	617	28/01/2026	A	
12c	83	53.78545	-2.965401	NE	336470	432665	612	28/01/2026	A	
12d	84	53.78154	-2.965804	N	336445	432235	569	28/01/2026	A	

Appendix B - Ground Image Log: Location 10 (Main Drain Bank Face)

B.1 Purpose of This Log

This table presents a chronological log of ground-based photographic observations recorded at Location 10, documenting the evolution of bank-face discharge, seepage expression, and associated sediment staining along the Main Drain. Images were acquired repeatedly between January and February 2026 under varying water-level conditions, allowing temporal comparison of surface expression, discharge point migration, and bank response.

Each entry records the figure reference used in the main body of the report, image acquisition date, source filename, observed relative water level at the time of capture, and a concise description of the visible features. The log is intended to provide transparent traceability between individual observations and the interpretive discussion presented in Sections 4.10 and 10.

This appendix supports the interpretation that observed seepage and sediment expression at Location 10 represent an evolving and dynamic subsurface process, rather than a static or isolated surface phenomenon.

Ground Image Log – Location 10 (Main Drain bank face)

Fig	Date	File name	Water level	Notes
64	04/01/2026	20260104_145602	Low	Two discharge openings visible; orange sediment present above tyre and to the right of the larger sinus.
65	12/01/2026	IMG-20260112-WA0021	Medium	Larger sinus remains visible; base of smaller opening submerged.
66	16/01/2026	IMG-20260116-WA0003	Low	Fresh sediment observed to the right of the larger sinus, with a small new opening visible.
67	19/01/2026	IMG-20260119-WA0001	High	Larger sinus remains visible; base of smaller opening submerged by elevated water level.
68	02/02/2026	IMG-20260202-WA0000	Medium	Left-hand seep closed; sediment emergence now higher on bank. New staining to the left with two distinct exit points.
69	04/02/2026	IMG_20260204_121058	Low	New sinus and staining observed south of original discharge area; localised bank erosion visible.
70	04/02/2026	IMG_20260204_121056	Low	Intermediate view of bank face showing seepage alignment and surface wetness.
71	04/02/2026	IMG_20260204_121056	Low	Close-range detail view of seepage, illustrating fine-scale flow patterning and multiple emergence points.

Water level descriptors (Low / Medium / High) are relative and qualitative, based on visual assessment at the time of observation.

Appendix C - LiDAR Processing Workflow and Interpretation Controls

C.1 Purpose of LiDAR Analysis

LiDAR elevation data were used in this report to provide spatial and temporal context for observed surface features. The purpose of the LiDAR analysis was to identify relative elevation change, spatial coherence, and geometric patterns across the study area, and to compare these with surface expressions documented through aerial and ground-based observations.

LiDAR data are not used in this report to infer causation, depth of change, subsurface structure, or deformation mechanisms. Interpretation is limited to relative surface elevation differences and their spatial relationship to independently observed surface features.

C.2 Data Sources

The analysis uses publicly available airborne LiDAR datasets for two time points:

• 2018 LiDAR dataset
• 2022 LiDAR dataset

Both datasets were supplied in raster format and projected in OSGB36 / British National Grid coordinates. Resolution and vertical accuracy are consistent with national LiDAR products intended for landscape-scale assessment rather than engineering design.

C.3 Pre-processing and Alignment

Prior to differencing, the following steps were undertaken:

• Verification that both datasets used the same coordinate reference system
• Confirmation of consistent raster resolution and grid alignment
• Visual inspection for edge artefacts, voids, and acquisition anomalies

No interpolation, smoothing, or terrain modelling was applied. Processing was limited to alignment and subtraction of the original datasets.

C.4 Elevation Differencing Method

Relative elevation change was calculated by subtracting the 2018 elevation raster from the 2022 elevation raster on a cell-by-cell basis:

Elevation change = 2022 surface elevation minus 2018 surface elevation

The resulting raster represents relative surface elevation gain or loss over the 2018-2022 period.

Positive values indicate relative elevation increase.
Negative values indicate relative elevation decrease.

C.5 Contour Generation and Interval Selection

To aid interpretation of low-magnitude surface change, contours were generated from the elevation-difference raster using a fixed interval of 0.03 m (3 cm).

This interval was selected to balance the following considerations:

• sufficient sensitivity to resolve subtle but spatially coherent surface features
• avoidance of excessive visual clutter that can obscure pattern recognition
• computational stability when applied consistently across multiple locations

The contour spacing does not imply precision beyond the underlying data resolution and is used solely as a visual aid to illustrate geometry, continuity, and relative change.

C.6 Value Masking and Surface Water Considerations

Extreme positive and negative values at the tails of the differenced raster were masked where appropriate. This was done to prevent visual dominance by outliers that can arise from:

• standing surface water
• water-surface reflection artefacts
• seasonal vegetation differences
• acquisition-condition variability

Masking was applied conservatively and uniformly, with the intent of clarifying spatial patterns rather than emphasising magnitude. Masked values do not affect the underlying interpretation of relative change within the retained range.

Surface water is recognised as a known limitation of airborne LiDAR elevation differencing. Areas of open water, ponding, or saturated ground can produce unreliable elevation signals. Where such effects are visible, they are identified explicitly in figure captions and distinguished from genuine surface deformation.

C.7 Visualisation Controls

To ensure consistency and avoid over-interpretation:

• Colour scales were kept consistent across locations
• Low-magnitude changes were retained rather than thresholded
• Bounding boxes were used only for orientation and spatial reference
• Contours were overlaid without smoothing or manual editing

In selected cases, measurement tools were used to estimate the order of magnitude of relative elevation change (e.g. ~0.12 m or ~0.15 m). These values are provided for scale only and are not used to infer volume, rate, or mechanism.

C.8 Limitations

The LiDAR analysis has the following acknowledged limitations:

• it cannot resolve subsurface processes or depth of change
• it cannot distinguish between different causal mechanisms
• it is sensitive to surface water and vegetation conditions
• it is not suitable for determining engineering tolerances or failure thresholds

For these reasons, LiDAR results are interpreted only in conjunction with aerial imagery and ground observations, and never in isolation.

C.9 Role Within the Evidence Hierarchy

Within this report, LiDAR elevation differencing functions as secondary corroborative evidence. It is used to:

- identify spatial coherence across locations
- demonstrate persistence of surface change over multi-year periods
- provide landscape-scale context for localised observations

Primary evidential weight is placed on repeat ground observations and time-series aerial imagery. LiDAR is used to support, contextualise, and test consistency, not to substitute for direct observation.

C.10 Summary

The LiDAR processing and visualisation workflow applied in this report is deliberately conservative. Contour spacing, masking, and visual controls were selected to enhance clarity without exaggeration, and to reflect the limitations of the underlying data. When used alongside surface observations, the LiDAR analysis provides a robust and transparent basis for identifying spatially coherent and persistent ground response across the study area.

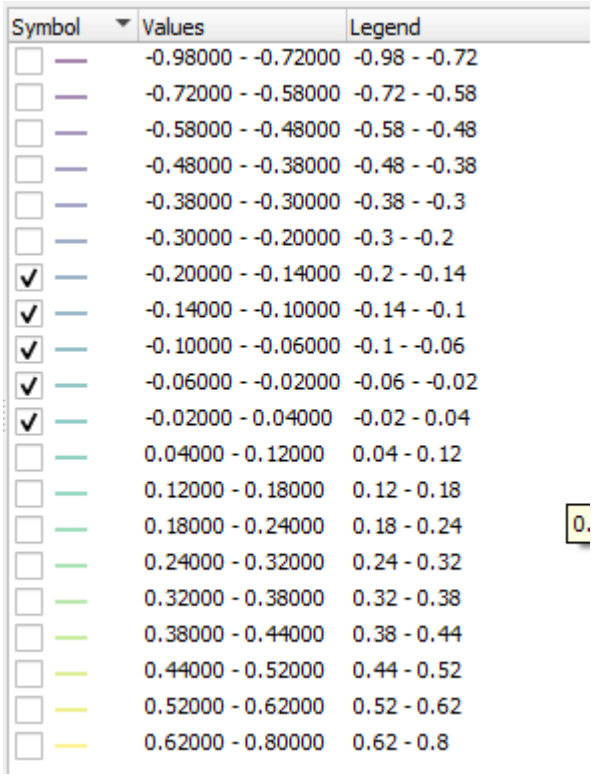

LiDAR elevation differencing was visualised using 3 cm contours with conservative masking of extreme values to balance clarity, sensitivity, and known limitations associated with surface water and acquisition variability.

Appendix D: Image Provenance, File Handling, and RAW/JPEG Use

D.1 Purpose of Image Documentation

Aerial and ground-based imagery form a primary component of the evidential record presented in this report. Images are used to document surface conditions, track temporal change, and provide visual context for features identified through LiDAR analysis and field observation.

This appendix documents image provenance, file handling practices, and the use of RAW and JPEG formats to ensure transparency, reproducibility, and appropriate interpretation of visual evidence.

D.2 Image Acquisition

All images included in this report were captured by the author using consumer-grade unmanned aerial vehicles (UAVs) and handheld mobile devices.

Image acquisition dates, approximate locations, viewing direction, and platform type (aerial or ground-based) are recorded in the Location Index and associated image logs. Where relevant, UAV image identifiers (e.g. DJI_####) or device-generated filenames are retained to preserve traceability.

No third-party imagery has been modified or repurposed beyond standard citation and contextual use (e.g. Google Earth time-series imagery).

D.3 RAW and JPEG Image Formats

Where available, aerial images were captured in RAW (DNG) format alongside compressed JPEG outputs.

RAW (DNG) files preserve the full dynamic range and colour information recorded by the sensor at the time of capture. These files retain subtle tonal variation, staining, and low-contrast features that may be reduced or lost during JPEG compression.

JPEG images included in the report are derived either directly from the camera or from RAW files using default conversion settings. JPEGs are used for document presentation due to file size and compatibility considerations.

D.4 Image Processing and Handling

Image processing was deliberately minimal and limited to the following actions:

- global exposure adjustment where required for legibility
- cropping for framing and orientation
- resizing for document layout

No localised enhancement, selective editing, feature exaggeration, or compositing was applied. No elements were added, removed, or repositioned within any image.

Processing was applied uniformly and conservatively to preserve the original appearance of surface features.

D.5 RAW-JPEG Differences and Interpretation

In several cases, features such as red/orange staining, fine sediment patterns, surface films, or subtle moisture contrasts are more clearly visible in RAW imagery than in JPEG exports. This difference reflects the limitations of JPEG compression rather than post-processing manipulation.

Where such differences are relevant, they are noted explicitly in figure captions or accompanying text. The presence or absence of a feature in a compressed image is not treated as definitive evidence of its existence or non-existence.

RAW files are retained as the authoritative record and can be re-examined if required to clarify ambiguous features or tonal variation.

D.6 Image Selection and Representativeness

Images included in the report were selected to illustrate features already identified through repeated observation, time-series comparison, or spatial correlation with other datasets.

Images are not presented as isolated or exceptional examples. Where possible, features are shown from multiple viewpoints, dates, or scales (overview, intermediate, and close-range) to reduce the risk of misinterpretation.

The report does not rely on a single image to establish any conclusion.

D.7 Metadata and Traceability

Where available, image metadata including date, approximate location, and orientation have been retained. For privacy, safety, and document compatibility reasons, full EXIF datasets are not embedded within the report but are retained in original files.

Spatial referencing for aerial imagery is approximate and used for contextual alignment rather than precise measurement.

D.8 Limitations

Imagery used in this report has the following limitations:

- consumer-grade sensors
- variable lighting and seasonal conditions
- compression artefacts in JPEG formats
- perspective distortion in oblique views

These limitations are acknowledged and mitigated through the use of multiple data sources, repeat observations, and corroboration with LiDAR elevation differencing.

D.9 Role Within the Evidence Hierarchy

Imagery functions as primary observational evidence within this report, supported by LiDAR analysis and spatial indexing. Images are used to document surface expression, temporal change, and geometric relationships, not to infer subsurface mechanisms or quantitative deformation.

Interpretation is grounded in pattern recognition across datasets rather than reliance on individual images or isolated visual cues.

D.10 Summary

Image acquisition and handling practices in this report prioritise transparency, traceability, and restraint. The use of RAW imagery alongside JPEG presentation ensures that subtle surface features are not lost to compression, while conservative processing preserves the integrity of the original observations. Together with spatial indexing and repeat documentation, this approach provides a reliable visual record suitable for regulatory and technical review.

Appendix E: Terminology and Descriptive Language Controls

E.1 Purpose of Terminology Controls

This report documents surface and near-surface observations within a complex, low-lying, drainage-dependent landscape. To ensure clarity, neutrality, and evidential robustness, specific terminology controls have been applied throughout.

The purpose of this appendix is to clarify how descriptive terms are used, to distinguish observation from interpretation, and to prevent diagnostic or causal inference being implied where none is intended.

E.2 Descriptive Versus Interpretive Language

All terms used in the main body of the report are intended to describe observable surface expressions rather than to diagnose subsurface mechanisms, material properties, or causes.

Descriptions are based on visible geometry, spatial relationships, tonal variation, texture, persistence, and temporal change. Interpretive or process-based conclusions are explicitly avoided unless clearly stated as contextual or comparative.

Where interpretive framing is used, it is limited to pattern recognition across multiple observations and datasets, rather than attribution of cause.

E.3 Use of Key Terms

The following terms are used consistently and descriptively throughout the report:

• seepage
Used to describe visible emergence or movement of water at the ground surface or bank face. The term does not imply groundwater source, hydraulic head, pressure conditions, or subsurface pathway.

• staining
Refers to visible colouration (e.g. red, orange, brown) on soil, sediment, vegetation, or water surfaces. No chemical composition, origin, or contamination status is inferred unless explicitly stated.

• depression / subsidence
Used to describe localised surface lowering relative to surrounding ground. Where supported by LiDAR elevation differencing, values are provided for scale only and are not used to infer volume, depth, rate, or mechanism.

• deformation / ground response
Used to describe changes in surface geometry, alignment, or texture over time. These terms do not imply failure, instability, or irreversible damage unless explicitly stated.

• bank instability / erosion
Used to describe observable bank geometry change, material loss, undercutting, or collapse. No assumption is made regarding trigger, rate, or future progression.

• preferential pathway / alignment
Used to describe repeated or linear spatial patterns visible across imagery or datasets. The term does not assert a specific subsurface conduit, fracture, or material property.

E.4 Avoidance of Diagnostic Terminology

The report deliberately avoids diagnostic, mechanistic, or regulatory trigger terminology, including but not limited to:

• failure
• contamination
• pollution
• liquefaction
• piping (except where explicitly qualified as morphological resemblance)
• structural defect
• breach (unless referring to visible loss of containment)

Where similar terms appear in quoted material or external references, they are contextualised and not adopted as findings of this report.

E.5 Treatment of Ambiguity

Where surface features could plausibly have multiple explanations (e.g. natural seepage, drainage interaction, soil heterogeneity, or infrastructure influence), the report adopts neutral phrasing and avoids exclusionary language.

Ambiguity is treated as an observation in itself rather than a deficiency. Where uncertainty exists, it is stated explicitly rather than resolved through assumption.

E.6 Consistency Across Sections

Terminology has been applied consistently across locations, figures, and summaries to avoid inadvertent escalation or dilution of meaning between sections.

Where similar features recur in different settings, the same descriptive language is used unless a clear observational distinction is present.

E.7 Relationship to Regulatory Interpretation

The descriptive terminology used in this report is not intended to substitute for regulatory classification, statutory assessment, or compliance determination.

The report provides observational evidence and spatial context to support informed review by competent authorities. Any regulatory interpretation, classification, or response lies outside the scope of this document.

E.8 Summary

Terminology within this report has been selected and applied to prioritise accuracy, neutrality, and evidential clarity. Descriptive language is used to document what is observed, where it occurs, and how it changes over time, without asserting cause or consequence.

These controls ensure that the report remains focused on observable ground behaviour and surface expression, providing a reliable foundation for further assessment without pre-empting interpretation or responsibility.

Appendix F: Scope, Exclusions, and Use of This Document

F.1 Purpose and Scope

This document presents a structured, evidence-led record of observed surface and near-surface ground conditions within a defined study area surrounding Preston New Road. Its scope is limited to the documentation, spatial contextualisation, and temporal comparison of observable surface expressions, supported by aerial imagery, ground photography, and LiDAR elevation differencing.

The report is intended to inform understanding of surface behaviour and ground response within a low-lying, drainage-dependent landscape. It does not seek to provide a definitive explanation of subsurface mechanisms, nor does it assert causation, liability, or regulatory non-compliance.

F.2 What This Report Does

This report:

- Documents observable surface features, their spatial distribution, and their evolution over time
- Integrates multiple datasets to provide corroborative spatial and temporal context
- Identifies patterns of ground response across different land uses and infrastructure settings
- Highlights limitations in detectability, classification, and oversight based on observed behaviour
- Provides a descriptive evidence base to support informed review by competent authorities

All conclusions are derived from observed data and are framed to reflect uncertainty where it exists.

F.3 What This Report Does Not Do

This report does not:

• Attribute cause or mechanism to observed features
• Diagnose subsurface conditions, material properties, or failure modes
• Assign responsibility, liability, or fault to any party
• Assess compliance with statutory thresholds or permit conditions
• Substitute for geotechnical investigation, intrusive testing, or regulatory determination
• Predict future behaviour, rates of change, or risk outcomes

Any inference beyond the descriptive and contextual scope of this report lies outside its intended use.

F.4 Treatment of Evidence and Uncertainty

All datasets used in this report are subject to known limitations, including resolution constraints, environmental interference, and temporal gaps. These limitations are acknowledged explicitly where relevant.

Uncertainty is treated as an inherent component of complex ground-water-surface systems rather than as an error to be eliminated. Where interpretation is uncertain or ambiguous, this is stated directly, and no attempt is made to resolve uncertainty through assumption.

F.5 Use and Citation of This Document

This document is intended to be read and interpreted as a whole. Selective quotation, extraction of individual figures, or isolation of statements from their accompanying context, while not forbidden, may alter the interpretation of the findings.

Figures, summaries, and descriptive statements should be considered in conjunction with the associated location narratives, methodological appendices, and terminology controls.

Any secondary use of this document should preserve the distinction between observation and interpretation established throughout.

F.6 Relationship to Other Assessments

This report does not replace or supersede formal regulatory assessments, environmental monitoring programmes, or engineering evaluations. It is intended to complement such work by providing observational evidence that may inform further investigation, review, or monitoring design.

Where discrepancies arise between this report and other assessments, such differences should be examined through additional data collection or interdisciplinary review rather than through dismissal or assumption.

F.7 Closing Statement

This document presents evidence of observable, evolving ground and surface behaviour within the study area. It does so without asserting cause, consequence, or fault, and without exceeding the limits of the available data.

Its value lies in documenting what is present, how it changes, and where it occurs, thereby supporting informed consideration of whether existing monitoring, oversight, and interpretive frameworks are adequate for the conditions observed.

Appendix G: Experimental Seepage Erosion and Channelisation Framework (after Berhanu et al., 2012)

This appendix provides contextual experimental reference material drawn from Berhanu et al. (2012), which investigated seepage-driven erosion and channelisation in granular and weakly cohesive media under controlled laboratory conditions. The material is included to support qualitative comparison with surface expressions documented in the present report, particularly where repeated seepage emergence, channel migration, bank instability, and progressive surface adjustment are observed in field settings.

The figures reproduced here illustrate fundamental process geometries associated with seepage erosion, including the development of subsurface flow pathways, emergence of concentrated discharge points, channel widening and bifurcation, and episodic bank collapse. These processes are shown to evolve over time in response to hydraulic gradients, boundary conditions, and surface–subsurface interactions, rather than occurring as single, instantaneous events.

The inclusion of this material is not intended to imply scale equivalence, material equivalence, or direct mechanistic attribution between laboratory experiments and the field observations presented elsewhere in this report. Instead, the figures are provided as conceptual analogues to assist interpretation of observed surface forms and behaviours, particularly where those behaviours exhibit migration, reorganisation, or temporal progression consistent with seepage-controlled erosion processes.

All figures in this appendix are reproduced or adapted from Berhanu et al. (2012) and retain their original experimental context. Interpretation within this report remains descriptive and comparative only, in keeping with the evidential and interpretive limits set out in Sections 1.3 and Appendix F.

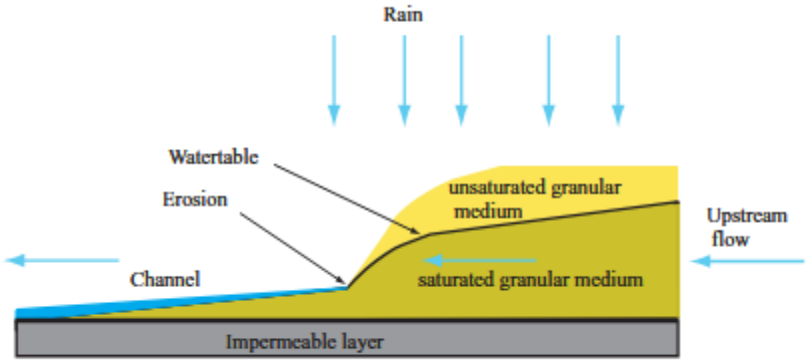

FIG. 1. (Color online) A schematic cross-sectional view of the geometry of seepage erosion. Water moves inside the bed from upstream (right) to downstream (left) direction. The water table is the surface separating medium saturated by water from the unsaturated medium and intersects the granular surface where the water flow emerges at the surface. Grains can be removed by water flowing near the surface leading to headward growth in the upstream direction.

Figure G-1.

Conceptual cross-section illustrating seepage erosion geometry, including subsurface flow convergence, emergence at the surface, and headward channel growth (after Berhanu et al., 2012).

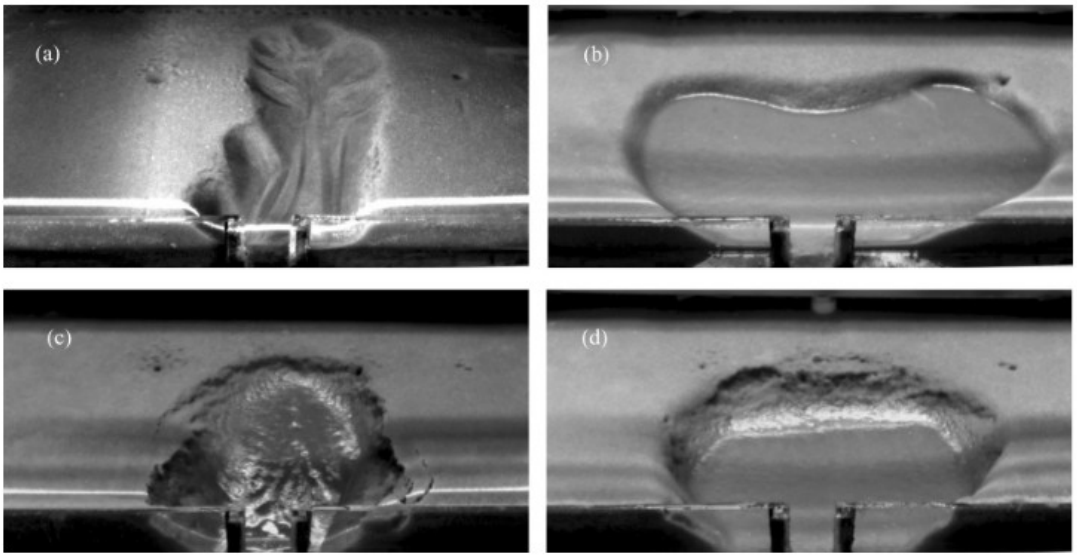

FIG. 4. Images of the four kinds of channels observed in the experiments. (a) An elongated channel fed by a flow from a reservoir at the back of the bed after $t = 916$ min with $d_{\text{outlet}} = 4$ cm, $\delta_H = 5$ cm, and no rainfall ($P = 0$). (b) A wider bifurcated channel fed by rain ($P_1 \sim 1.04 \times 10^{-4}$ m s^{-1}) is observed with $d_{\text{outlet}} = 4$ cm ($\delta_H = 5$ cm, $t = 595$ min). (c) An elongated deeper channel with steeper banks is observed with $d_{\text{outlet}} = 8.0$ cm ($P = 0$, $\delta_H = 6.8$ cm, $t = 311$ min). (d) The channel is deeper with $d_{\text{outlet}} = 8.0$ cm and wider with rain ($P = P_1$, $\delta_H = 2$ cm, $t = 240$ min).

Figure G-2.

Experimental images showing different seepage-driven channel forms produced under varying hydraulic and rainfall conditions, including elongated, widened, and deepened channels (after Berhanu et al., 2012).

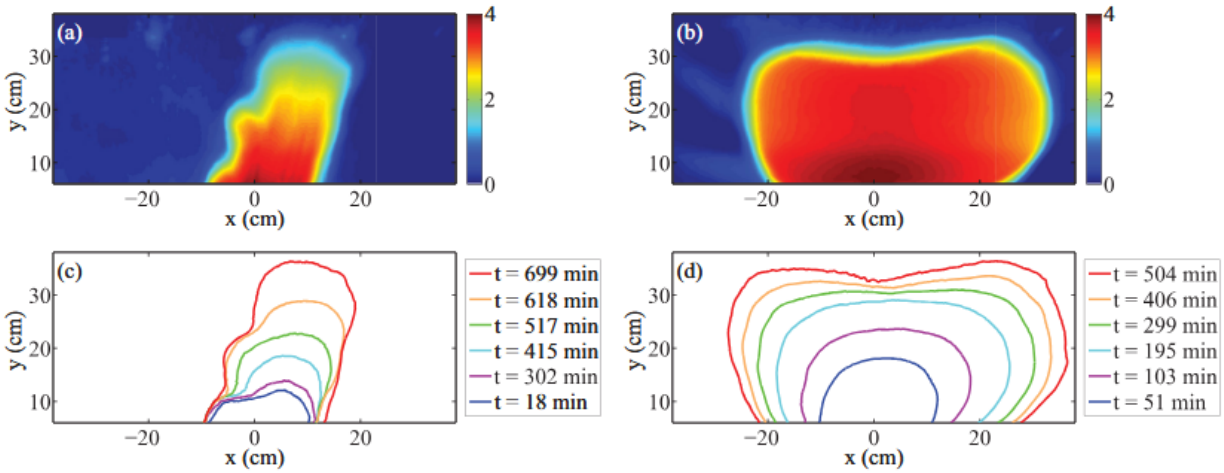

FIG. 5. (Color online) Comparison of channels in a shallow channel regime where the capillary rise is of order of the channel depth. (a) Depth map of the channel observed after $t = 677$ min with $\delta_H = 5$ cm, $P = 0$, and $d_{\text{outlet}} = 4$ cm. Depth is indicated with a scale in centimeters measured from the initial flat bed. (b) Depth map of channel observed after $t = 300$ min with $P_1 \sim 1.04 \times 10^{-4}\,\text{m s}^{-1}$, $\delta_H = 0.9$ cm, and $d_{\text{outlet}} = 4$ cm. (c,d) The corresponding channel shape evolution for the depth $d(x, y) = 1$ cm contour increase in length with time.

Figure G-3.

Depth maps and contour evolution illustrating temporal development and widening of seepage-driven channels under reservoir-fed and rainfall-fed conditions (after Berhanu et al., 2012).

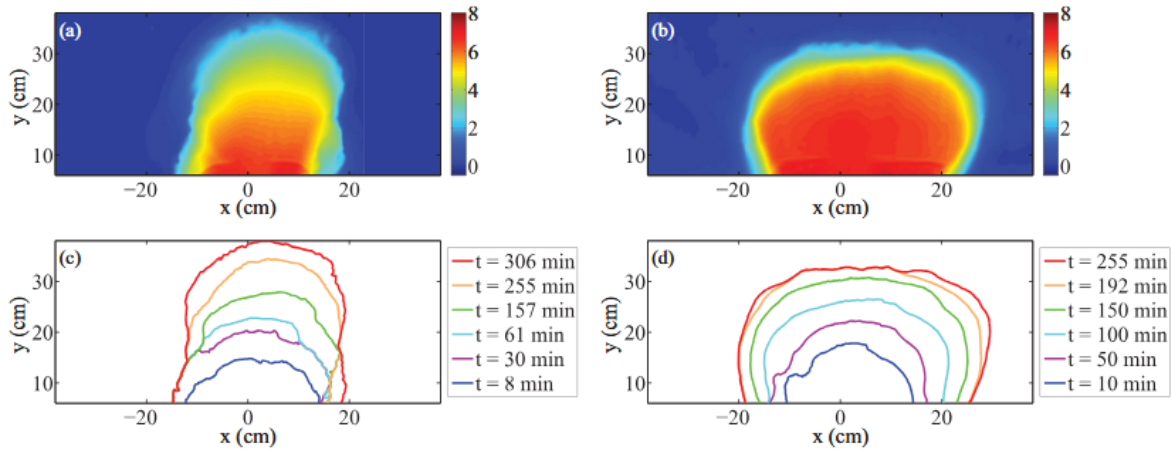

FIG. 7. (Color online) Comparison of channel shape in the regime where $d_{\text{outlet}} > d_{\text{cap}}$ and significant layer of unsaturated cohesive bed layer is present. (a) Depth map of channel observed after $t = 306$ min with $d_{\text{outlet}} = 8.0$ cm, $\delta_H = 6.8$ cm, and $P = 0$. (b) Depth map of channel observed after $t = 225$ min with $d_{\text{outlet}} = 8.0$ cm, $\delta_H = 2.0$ cm, and $P = P_1$. (c,d) The corresponding channel shape evolution for the depth $d(x, y) = 1$ cm contour. The contours increase in length with time.

Figure G-4.

Comparison of channel shape evolution where outlet diameter exceeds capillary rise and an unsaturated cohesive layer is present, showing progressive lateral and upstream growth (after Berhanu et al., 2012).

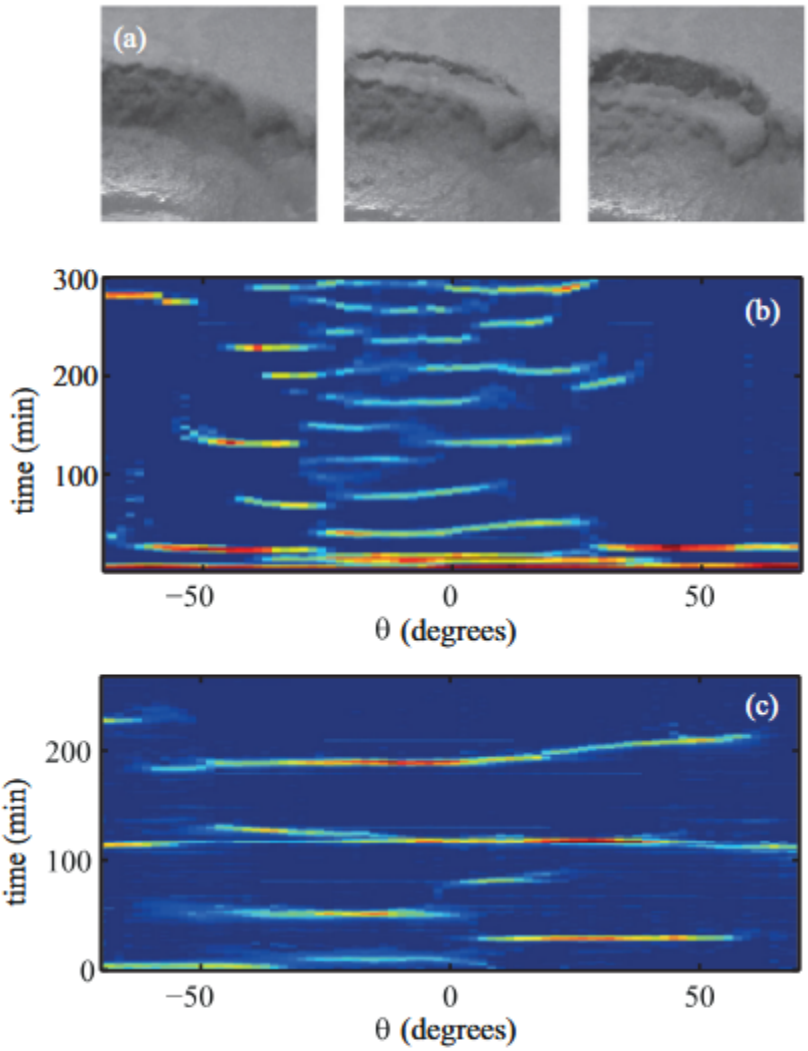

FIG. 9. (Color online) (a) Sequence of images illustrate a channel bank collapse. A crack initially appears and breaks a block, which falls inside the channel over the time scale of a minute. (b) The spatiotemporal development of avalanches as a function of the angle θ and time (b) in case of flow from reservoir and (c) in case with local rain (the experimental parameters are the same as in Fig. 7). The color scale is in arbitrary units and corresponds to the temporal derivative of the distance from the contour at $d(x,y) = 1$ cm and origin.

Figure G-5.

Sequence illustrating bank collapse and spatiotemporal evolution of avalanching during seepage-driven erosion, highlighting episodic rather than continuous adjustment (after Berhanu et al., 2012).

Appendix H - Contextual Spatial Overlay: Independent Subsurface Reference Geometry and LiDAR Elevation Change

This appendix presents a spatial overlay of independently derived subsurface reference features and LiDAR-derived surface elevation change for contextual completeness. The material is included to document the geographic relationship between previously published subsurface operational geometries and the surface patterns discussed elsewhere in this report. The figure is provided for contextual reference only and does not form part of the evidential basis for the findings of this report.

The figure is not relied upon as evidential support for the observations or interpretations presented in the main body of the report and is not used to infer causation, mechanism, or operational impact. Its inclusion reflects transparency regarding available spatial datasets relevant to the study area.

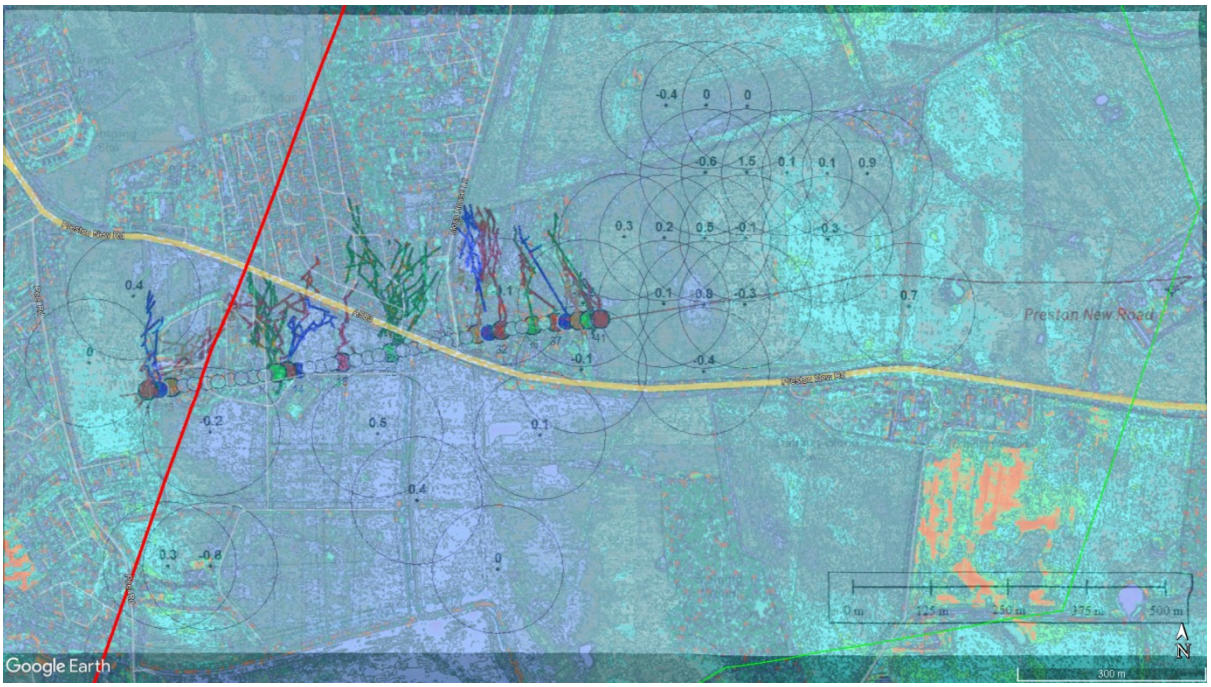

Figure H-1 - Spatial overlay of previously published subsurface operational reference geometry and unprocessed LiDAR-derived surface elevation change (2018–2022).

The figure overlays previously documented subsurface operational reference features (including stimulation stage locations and deformation indicators, reproduced from earlier work) onto differential LiDAR-derived surface elevation change between 2018 and 2022.

The LiDAR data are displayed without enhancement, thresholding, or classification and are used solely to visualise spatial distribution and clustering of relative elevation change. No inference is made regarding causation, magnitude, depth, or mechanism of deformation.

The subsurface reference features are included for geographic orientation and comparative context only, allowing visual assessment of map-scale co-location between surface elevation patterns and independently defined subsurface intervention zones. The figure is not used to support causal attribution and serves a contextual role consistent with the secondary evidential status assigned to LiDAR datasets in this document.

Appendix I - Table of Figures

Figure 1 - Regional context of study area prior to 2011 7
Figure 2 - Study area looking west (Google Earth, October 2024) 8
Figure 3 - Broad topographic context of the study area (historical elevation data) 11
Figure 4 - Topographic context looking west. 11
Figure 5 - Contemporary topographic projection and persistent low-gradient geometry (accessed 2026) 12
Figure 6 - Location 1: Site context and surrounding landscape (Google Earth image, 06/24) 14
Figure 7 - Location 1: LiDAR elevation change context (2018-2022) 15
Figure 8 - Location 1a Bank morphology and adjacent field context (28/01/2026) 16
Figure 9 - Location 1a: Detail of seepage, staining, and surface water characteristics. 17
Figure 10 - Location 2: Site context and image positions (Google Earth, June 2024) 18
Figure 11 - Location 2: LiDAR elevation change context (2018-2022) 19
Figure 12 - Location 2A: Aerial image showing bank condition and channel context (28/01/2026) 20
Figure 13 - Location 2A: Aerial zoomed view of bank erosion and seepage at the waterline (28/01/2026) 21
Figure 14 - Location 2B: Aerial image facing northwest along the watercourse (28/01/2026) 22
Figure 15 - Zoomed view derived from ground-based imagery at Location 2. 23
Figure 16 - Location 3: Aerial overview of bank and adjacent field condition. (Google Earth; 10/2024) 25
Figure 17 - Location 3: LiDAR elevation change context (2018-2022) 26
Figure 18 - Location 3A: Aerial image showing bank condition and localised bank-face opening (28/01/2026) 27
Figure 19 - Location 3A: Aerial zoomed view derived from above UAV RAW imagery. 28
Figure 20 - Location 3B: Aerial image showing bank-face opening with associated staining at the waterline (28/01/2026) 29
Figure 21 - Zoomed aerial view showing the bank-face opening and associated red/orange staining at the waterline at Location 3B. 30
Figure 22 - Location 3C: Site context and spatial relationship (aerial image 28/01/2026) 31
Figure 23 - Location 3C: Bank seepage and erosion detail (aerial image) 32
Figure 24 - Site overview and image orientation (Google Earth, 06/2024) 34
Figure 25 - Location 4: LiDAR elevation change context (2018-2022) 35
Figure 26 - Location 4a, overview and surface context (22/10/2018) 36
Figure 27 - Magnified view of the same area, identifying the position of the ground-based photograph presented in Figure 28. 37
Figure 28 - Ground-level surface disturbance at Location 4 (22/10/2018) 38
Figure 29 - Aerial image (28/01/2026) of the southern section of the M55 culvert at the Main Drain crossing. 39
Figure 30 - Magnified aerial view of the motorway bridge embankment at the Main Drain crossing. 40
Figure 31 - Aerial view of ground depressions SSE of the motorway bridge. 41
Figure 32 - Zoomed aerial view showing fluid-filled depressions and fence-line continuity. 42
Figure 33 - Temporal comparison of ground condition prior to and following depression formation. 42
Figure 34 - Location 5: Aerial overview (May 2025) 44
Figure 35 - Location 5: LiDAR elevation change context (2018-2022) 44
Figure 36 - Location 5a, Aerial view of linear surface features adjacent to tributary 45
Figure 37 - Location 5a, Localised bank disturbance at tributary (DJI_0414) 46

Figure 38 - Location 5a, Detail view of surface features and infrastructure deformation (DJI_0414) 47
Figure 39 - Location 5b: ponding and bank-adjacent staining near the motorway corridor. 48
Figure 40 - Location 6: Aerial overview and image orientation (28/01/2026) 49
Figure 41 - Location 6: LiDAR elevation change context (2018-2022) 50
Figure 42 - Aerial view of Location 6a facing northeast (28/01/2026)..... 51
Figure 43 - Overview of Location 7 and surface context (Google Earth, 08/2025)..... 53
Figure 44 - Location 7: LiDAR elevation change context (2018-2022) 54
Figure 45 - Location 7: Bank erosion and channel-margin instability along CBB. 55
Figure 46 - Intervening fields between Locations 6 and 7 (Google Earth, 04/2025). 56
Figure 47 - Bridging fields between Locations 6 and 7: LiDAR elevation change context (2018-2022)..... 57
Figure 48 - Oblique aerial view of intervening fields prior to observed deformation (24/08/2017). 58
Figure 49 - Oblique aerial view of ground deformation within an intervening field between Locations 6 and 7 (28/01/2026)..... 59
Figure 50 - Persistent groundwater staining in bridging fields between Locations 6 and 7. 60
Figure 51 - Top-down Google Earth imagery (06/2018) showing the setting of Location 8..... 61
Figure 52 - Location 8: LiDAR elevation change context (2018-2022) 62
Figure 53 - Reomved in 1.1..... 63
Figure 54 - Opposite-direction view of embankment deformation at Location 8c. 64
Figure 55 - Pale mineral residue within the depression at Location 8d. 65
Figure 56 - Location 9 context and setting (Google Earth, 05/2020)..... 67
Figure 57 - LiDAR elevation change context at Location 9 (2018-2022) 67
Figure 58 - Location 9(a) - Ground photograph of verge surface irregularities at Location 9 (23/05/2025)..... 68
Figure 59 - Location 9 (b) Ground photograph showing flat surfaced feature within Location 9. 68
Figure 60 - Location 9(c) Ground photograph showing surface mounding and redistribution at Location 9 (08/01/2026)..... 69
Figure 61 - Top-down Google Earth imagery showing Location 10 in relation to Location 9, Preston New Road, and the Main Drain corridor (06/2022). 70
Figure 62 - LiDAR elevation change context at Location 10 (2018-2022). 71
Figure 63 - Bank-face discharge at Location 10 (04/01/2026)..... 72
Figure 64 - Elevated water level partially occluding lower discharge points (12/01/2026)..... 73
Figure 65 - Receding water level with renewed sediment expression (16/01/2026). 74
Figure 66 - Elevated water level within the Main Drain (19/01/2026). 75
Figure 67 - Progressive change in bank-face configuration at Location 10 (02/02/2026). 76
Figure 68 - Ground photograph of Main Drain bank and staining (04/02/2026)..... 77
Figure 69 - Intermediate view of seepage feature shown in Figure 68. 78
Figure 70 - Close-range detail of seepage feature shown in Figure 69. 79
Figure 71 - Aerial imagery showing surface conditions at Location 10. 80
Figure 72 - Google Earth context and oblique imagery orientation (06/2024) 82
Figure 73 - LiDAR elevation differencing (2018-2022) for Location 11, with four sub-areas of interest delineated..... 83
Figure 74 - Location 11a - Pond overtopping and northward water expansion 84
Figure 75 - Location 11b - Ground surface expression aligned with LiDAR depression 85
Figure 76 - Location 11c - Seepage associated surface saturation and deformation northwest of the pond..... 86
Figure 77 - Location 11d - Bank collapse along Carr Bridge Brook, north of Location 11. 87
Figure 78 - Google Earth overview of Location 12 (10/2024)..... 89
Figure 79 - Location 12: Google Earth view overlaid with LiDAR elevation differencing (2018–2022)..... 89

Figure 80 - Location 12a: Aerial image looking east across fields south of the A583. 90
Figure 81 - Location 12b: Surface ponding and sediment staining within low-relief field. 91
Figure 82 - Location 12c: Surface disturbance and shallow water accumulation adjacent to the A583. 92
Figure 83 - Location 12d: Fluid-filled depression and associated vegetation stress. 93